The influence of counter ion and ligand methyl substitution on the solid-state structures and photophysical properties of mercury(ii) complexes with (E)-N-(pyridin 2-ylmethylidene)arylamines

Basu Baul, Tushar S ; Kundu, Sajal ; Mitra, Sivaprasad ; Höpfl, Herbert ; Tiekink, Edward R T ; Linden, Anthony

Abstract: Ten neutral monomeric, dimeric and polymeric mercury(II) complexes of compositions HgX2L (3, 8), [HgX2L]2 (1, 2, 4–6 and 7), [Hg(NO3)2L]n (9) and [Hg(N3)2L]2n (10) where X = chloride, bromide, iodide, nitrate and azide, and L = (E)-N-(pyridin-2-ylmethylidene)arylamine, are described. Compounds 1–10 were characterized by elemental analyses, and IR and 1H NMR spectroscopic studies. The solution-state photophysical properties of the complexes are highly dependent on the anions as seen in the fluorescence emission features. Single-crystal X-ray crystallography showed that the molecular complexes can aggregate into larger entities depending upon the anion coordinated to the metal centre. Iodide gives discrete monomeric complexes, chloride and bromide generate binuclear complexes formed through Hg–X–Hg bridges, while nitrate and azide lead to 1D coordination polymers. The significant differences in the observed aggregation patterns of the compounds indicate that the anions exert a substantial influence on the formation of the compounds. A further influence upon supramolecular aggregation is the presence of methyl substituents in L3 and L4, which generally enhances the probability of forming supramolecular interactions involving the five-membered C2N2Hg chelate rings in their crystal structures.

DOI: https://doi.org/10.1039/C2DT32283H

RSC Publishing Dalton Transactions

The influence of counter ion and ligand methyl substitution on the solid-state structures and photophysical properties of mercury(II) complexes with (E)-N-(pyridin-2-ylmethylene)arylamines

Journal:	*Dalton Transactions*
Manuscript ID:	DT-ART-09-2012-032283.R1
Article Type:	Paper
Date Submitted by the Author:	29-Oct-2012
Complete List of Authors:	Basu Baul, Tushar; North-Eastern Hill University, Chemistry; Chemistry Höpfl, Herbert; Universidad Autónoma del Estado de Morelos, Centro de Investigaciones Químicas Tiekink, Edward; University of Mayala, Department of Chemistry Linden, Anthony; University of Zurich, dInstitute of Organic Chemistry

The influence of counter ion and ligand methyl substitution on the solid-state structures and photophysical properties of mercury(II) complexes with (E)-N-(pyridin-2-ylmethylene)arylamines†

Tushar S. Basu Baul,*[a] Sajal Kundu,[a] Sivaprasad Mitra,[a] Herbert Höpfl,[b] Edward R. T. Tiekink,*[c] Anthony Linden[d]

Abstract

Ten neutral monomeric, dimeric and polymeric mercury(II) complexes of compositions HgX_2L (**3**,**8**), $[HgX_2L]_2$ (**1**,**2**,**4-6** and **7**), $[Hg(NO_3)_2L]_n$ (**9**) and $\{[Hg(N_3)_2L]_2\}_n$ (**10**) where X = chloride, bromide, iodide, nitrate and azide, and L = (*E*)-*N*-(pyridin-2-ylmethylidene)arylamine, are described. Compounds **1-10** were characterized by elemental analyses, and IR and ^{1}H NMR spectroscopic studies. The solution-state photophysical properties of the complexes are highly dependent on the anions as seen in the fluorescence emission features. Single-crystal X-ray crystallography showed that the molecular complexes can aggregate into larger entities depending upon the anion coordinated to the metal centre. Iodide gives discrete monomeric complexes, chloride and bromide generate binuclear complexes formed through Hg-X-Hg bridges, while nitrate and azide lead to 1D coordination polymers. The significant differences in the observed aggregation patterns of the compounds indicate that the anions exert a substantial influence on the formation of the compounds. A further influence upon supramolecular aggregation is the presence of methyl substituents in L^3 and L^4, which generally enhances the

probability of forming supramolecular π···π interactions involving the five-membered C_2N_2Hg chelate rings in their crystal structures.

[a]*Department of Chemistry, North-Eastern Hill University, NEHU Permanent Campus, Umshing, Shillong 793 022, India; E-mail: basubaul@nenu.ac.in, basubaulchem@gmail.com; Fax: +91-3642721000; Tel: +91-3642722626*

[b]*Centro de Investigaciones Químicas, Universidad Autónoma del Estado de Morelos, Av. Universidad 1001, 62209 Cuernavaca, Mexico; E-mail: hhopfl@uaem.mx; Fax, Tel: +52 777 3297997*

[c]*Department of Chemistry, University of Malaya, 50603 Kuala Lumpur, Malaysia; E-mail: Edward.Tiekink@gmail.com; Fax: +60 3 7967 4193; Tel: +60 3 7967 6775*

[d]*Institute of Organic Chemistry, University of Zurich, Winterthurerstrasse 190,CH-8057 Zurich, Switzerland; E-mail: alinden@oci.uzh.ch; Fax: +41 44 635 6812; Tel: +41-44 635 4228*

†Electronic supplementary information (ESI) available: CCDC reference numbers 892204–892213. For ESI and crystallographic data in CIF format see DOI: XXXXX

Introduction

The coordination chemistry of mercury(II) has been a focus of attention for many years owing to the significant toxicological effects exhibited by mercury upon living organisms. Mercury has a special affinity for sulphur and nitrogen over oxygen when these appear as potential ligator atoms in biochemically relevant or model compounds.[1] Despite their toxicity, mercury(II) compounds are still being used in various fields, such as in the paper industry, paints, cosmetics, preservatives, thermometers, manometers, energy-efficient fluorescent light bulbs and, to a limited extent, mercury batteries.[2] Nonetheless, reports of mercury compounds are disproportionately scarce compared with those describing zinc and cadmium, including in crystal engineering endeavours. Recent developments in the crystal engineering of metal-organic coordination polymers have produced many novel materials with various structural features and properties. Supramolecular structures that contain mercury(II) seem to have much more in common with low-valent main group elements than with transition metals, in part because they tend to form structures with low-coordinate linear or other distorted coordination geometries.[3] The spherical d^{10} configuration of Hg(II) is associated with a flexible coordination environment so that the geometries of these complexes can vary from linear to octahedral or even distorted hexagonal bipyramidal, and severe distortions from ideal coordination polyhedra occur easily. Furthermore, due to the general ability of d^{10} metal complexes, the formation of coordination bonds is reversible, which enables metal ions and ligands to rearrange during the supramolecular assembly to give highly ordered network structures. Consequently, mercury(II) can readily accommodate different kinds of architectures, and a selection of varying topological types of 1D, 2D and 3D polymers is given in refs. 2,4,5.

Recent attention has also been given to d^{10} metal complexes containing α-diimine ligands due to their luminescent and electroluminescent properties,[6-13] and their lower cost compared with the corresponding more commonly used rhenium(I),[14-17] ruthenium(II)[18-20] and osmium (II)[21-23] complexes. In this context, the luminescent and electroluminescent properties of alkynylmercury complexes and mercury bipyridine complexes have been examined.[24-28] Weak intermolecular $d^{10}\cdots d^{10}$interactions such as Au···Au and Hg···Hg contacts can play an important role in materials science and crystal engineering,[29-36] as their strength is comparable with those exhibited by hydrogen bonds and they are often responsible for the observed optical properties.[37-39] The formation of metal···metal and aryl···aryl interactions in the solid-state can cause a red shift in the emission band compared with that in solution phase.[40,41]

The solid-state structures of mercury(II) halide complexes with N-donor organic ligands (monodentate) have been thoroughly studied both by spectroscopic methods as well as by X-ray crystallography, which have demonstrated a broad variety of binding modes according to the characteristics of the ligands.[42-44] It is well known that mercury(II) is capable of forming various coordination modes with N,N-donor atoms when suitable ligands such as bipyridine (bpy), phenanthroline (phen) and their derivatives, *e.g.* 2,9-dimethyl-1,10-phenanthroline (dmph), are employed.[45,46] In the case of $Hg(bpy)I_2$, the presence of the bpy ligand leads to the formation of weakly associated dimers through Hg···I interactions, *i.e.* $[Hg(bpy)I_2]_2$, resulting in five-coordinate metal centres. In contrast, with phen and dmph, monomeric structures with distorted tetrahedral coordination geometries of composition $Hg(phen/dmph)I_2$ are observed.[45] This is as expected because the presence of bulky phen or dmph ligands inhibits aggregation. However, for $Hg(phen)_2Cl_2$ a six-coordinate complex with a distorted octahedral geometry was observed.[46] A previous investigation revealed that mercury(II) is capable of forming an extended polymeric

structure with 2-[(*E*)-2-(3-methylphenyl)-1-diazenyl]pyridine in which the ligand is monodentate *via* the pyridyl nitrogen, while modifying the structure of the ligand by changing the methyl group on the phenyl ring from the *m*- to the *p*-position resulted in a dimeric structure in which the 2-[(*E*)-2-(4-methylphenyl)-1-diazenyl]pyridine ligand is coordinated in a bidentate mode *via* the pyridyl nitrogen and one of the azo nitrogen atoms.[47]

In order to extend the current knowledge of the structural chemistry of mercury(II) compounds with N-donor ligands, attention is now directed towards the systematic synthesis and structural characterization of HgX_2 (X = chloride, bromide, iodide, nitrate and azide) complexes with (*E*)-*N*-(pyridin-2-ylmethylidene)arylamine derivatives (L^1-L^4, Chart 1), in order to analyze comprehensively the competition between anion X and ligand L for the coordination sites at the mercury(II) centre. Herein, we report the self-assembly and resulting structures of ten mercury(II) complexes (**1**-**10**) of varied composition, HgX_2L, $[HgX_2L]_2$, $[Hg(NO_3)_2L]_n$ and $\{[Hg(N_3)_2L]_2\}_n$, which have been characterized by means of IR and ^{1}H NMR spectroscopic studies, and for each of **2**-**10** additionally by single-crystal X-ray crystallography; the structure of **1** has been reported by others recently.[48] The solution-state photophysical properties of these compounds are also reported.

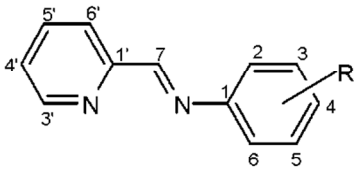

L

R = H (L^1), 2-CH_3 (L^2), 3-CH_3 (L^3), 4-CH_3 (L^4)

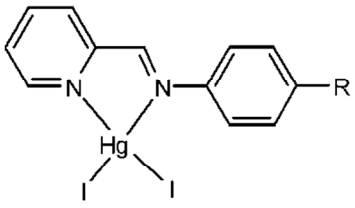

HgI_2L

R = H (**3**); R = CH_3 (**8**)

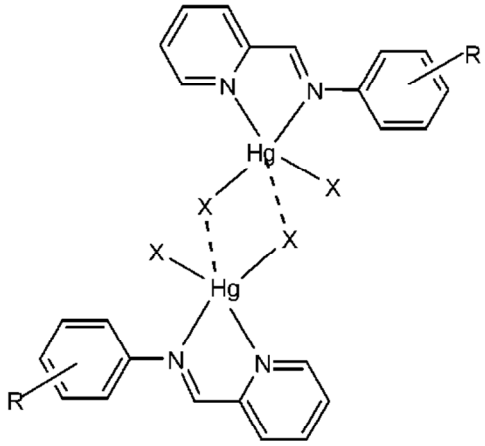

$[HgX_2L]_2$

R = H, X = Cl (**1**); R = **H**, X = Br (**2**); R = 2-CH_3, X = Cl (**4**); R = 3-CH_3, X = Cl (**5**); R = 4-CH_3, X = Cl (**6**); R = 4-CH_3, X = Br (**7**)

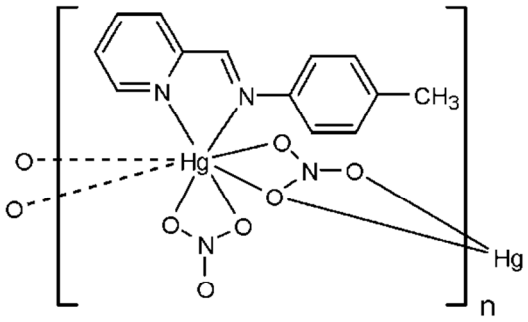

$[Hg(NO_3)_2L]_n$ (**9**)

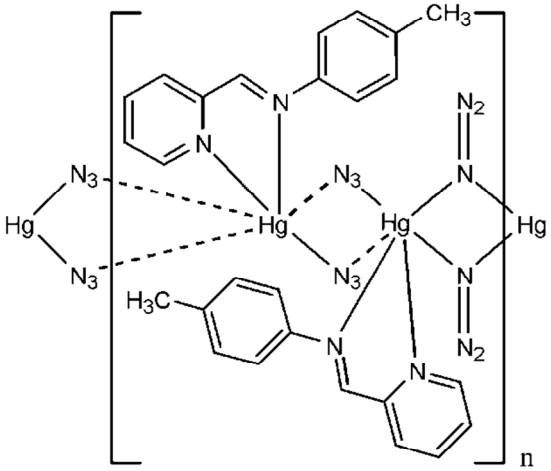

$\{[Hg(N_3)_2L]_2\}_n$ (**10**)

Chart 1 Chemical structures of ligands L^1-L^4 and the investigated mercury (II) complexes **1**-**10**.

Experimental

General considerations. ***Caution!*** *Compounds of mercury are highly toxic.*[49] *Care must be taken when handling samples, and appropriate disposal procedures are necessary.* All chemicals were used as purchased without purification: $HgCl_2$, pyridine-2-carboxaldehyde (Merck), $HgBr_2$,

HgI_2 (Fine Chemicals), $Hg(NO_3)_2$ (Sarabhai Chemicals), aniline (Sd Fine), *o*-/*m*-toluidine (Thomas Bakers) and *p*-toluidine (CDH). Solvents were purified by standard procedures and were freshly distilled prior to use. The (*E*)-*N*-(pyridin-2-ylmethylene)arylamine derivatives L^1-L^4 were prepared *in situ* from pyridine-2-carboxaldehyde and the corresponding aniline. Attempts to prepare crystalline (*E*)-*N*-(pyridin-2-ylmethylene)arylamine were unsuccessful and in all instances either an oil or a viscous liquid was isolated. Melting points were recorded in capillary tubes on a Scanca apparatus and are uncorrected. Elemental analyses were performed using a Perkin Elmer 2400 series II instrument. IR spectra in the range 4000-400 cm^{-1} were obtained on a Perkin Elmer Spectrum BX series FT-IR spectrophotometer with samples prepared as KBr discs (complex **9** also in nujol mull). The ^1H NMR spectra were recorded on a Bruker Avance II spectrometer and measured at 400.13 MHz. The ^1H chemical shifts were referenced to Me_4Si set at 0.00 ppm. Steady-state absorption spectra were recorded at ambient temperature in acetonitrile (spectroscopy grade, Merck) solution on a Perkin-Elmer model Lambda25 absorption spectrophotometer. Fluorescence spectra were obtained on a Hitachi model FL4500 spectrofluorimeter (with the excitation and emission slits fixed at 10 and 20 nm, respectively) and all spectra were corrected for the instrument response function. Quartz cuvettes of 10 mm optical path length received from Perkin Elmer, USA (part no. B0831009) and Hellma, Germany (type 111-QS) were used for measuring absorption and fluorescence spectra, respectively. Fluorescence quantum yields (ϕ_f) were calculated by comparing the total fluorescence intensity under the whole fluorescence spectroscopic range with that of a standard using the method described elsewhere.[50] The relative experimental error of the measured quantum yield was estimated within ±10%. Solution electrical conductivity measurements were made with a Wayne Kerr automatic precision bridge 6440B.

Synthesis of mercury compounds: HgX_2L (**3**, **8**), $[HgX_2L]_2$ (**1**, **2**, **4**-**7**), $[Hg(NO_3)_2L]_n$ (**9**) and $\{[Hg(N_3)_2L]_2\}_n$ (**10**)

Synthesis of dihalomercury(II) complexes (1-8)

The methods employed for the preparation of the dihalomercury(II) complexes (**1**-**8**) are very similar, so that the preparation of the dichloride derivative (**1**) is given in detail as a representative example.

Synthesis of $[HgCl_2L^1]_2$ (1). To a solution of pyridine-2-carboxaldehyde (0.20 g, 1.86 mmol) in ethanol (5 mL) was added a solution of aniline (0.17g, 1.86 mmol) in ethanol (10 mL). The mixture was stirred at ambient temperature for 30 min. To this reaction mixture, $HgCl_2$ (0.50 g, 1.84 mmol) in methanol (20 mL) was added drop-wise under stirring which resulted in the immediate formation of a yellow precipitate. Stirring was continued for 3 h and then the mixture was filtered. The residue was washed with methanol (3 x 5 mL) and dried *in vacuo*. The dried solid was dissolved by boiling in acetonitrile (40 mL) and filtered while hot. The filtrate, upon cooling to room temperature, afforded a yellow crystalline material. Yield 0.35 g (40%). M.p. 184-186 °C. Found: C, 31.70; H, 2.12; N, 6.10%. Calc. for $C_{24}H_{20}Cl_4Hg_2N_4$: C, 31.75; H, 2.22; N, 6.17%. Λ_m (CH_3CN): 5 $\Omega^{-1}cm^2mol^{-1}$. IR (cm^{-1}): 1633 ν_{asym}(C(H)=N); 1586, 1487, 1434 ν(C=N)py. ^{1}H-NMR (DMSO-d_6): δ 8.96 [s, 1H, H-7], 8.93 [d, 1H, H-3′], 8.18 [d, 1H, H-6′], 8.13 [dd, 1H, H-5′], 7.72 [dd, 1H, H-4′], 7.50 [m, 4H, H-2,3,5,6], 7.36 [t, 1H, H-4] ppm. The atom numbering scheme employed is shown in Chart 1.

Synthesis of $[HgBr_2L^1]_2$ (**2**). A similar synthetic procedure to that used for **1** was used except that $HgCl_2$ was replaced by $HgBr_2$, giving pale-yellow crystals from acetonitrile solution. Yield 46%. M.p. 184-186 °C. Found: C, 26.75; H, 1.80; N, 5.17%. Calc. for $C_{24}H_{20}Br_4Hg_2N_4$: C, 26.54; H, 1.86; N, 5.16%. Λ_m (CH_3CN): 4 $\Omega^{-1}cm^2mol^{-1}$. IR (cm^{-1}): 1646 ν_{asym}(C(H)=N); 1586, 1480, 1434 ν(C=N)py. ^{1}H-NMR (DMSO-d_6): δ 8.88 [s, 1H, H-7], 8.73 [d, 1H, H-3′], 8.04 [m, 2H, H-5′,6′], 7.65 [dd, 1H, H-4′], 7.40 [m, 5H, H-2,3,4,5,6] ppm.

Synthesis of $[HgI_2L^1]_2$ (**3**). A similar synthetic procedure to that used for **1** was used except that $HgCl_2$ was replaced by HgI_2, giving pale-yellow crystals from acetonitrile solution. Yield 44%. M.p. 170-172 °C. Found: C, 22.60; H, 1.68; N, 4.47%. Calc. for $C_{12}H_{10}HgI_2N_2$: C, 22.62; H, 1.58; N, 4.40%. Λ_m (CH_3CN): 3 $\Omega^{-1}cm^2mol^{-1}$. IR (cm^{-1}): 1639 ν_{asym}(C(H)=N); 1586, 1487, 1447 ν(C=N)py. ^{1}H-NMR (DMSO-d_6): δ 8.87 [s, 1H, H-7], 8.66 [d, 1H, H-3′], 8.06 [d, 1H, H-6′], 7.94 [dd, 1H, H-5′], 7.66 [dd, 1H, H-4′], 7.45 [m, 5H, H-2,3,4,5,6] ppm.

Synthesis of $[HgCl_2L^2]_2$ (**4**). A similar synthetic procedure to that used for **1** was used except that aniline was replaced by *o*-toluidine, giving pale-yellow crystals from acetonitrile solution. The crystalline sample contained crystals of two polymorphs. The estimate of the relative proportion of each polymorph in the sample was based on visual inspection of the crystals. The minor product (**4a**) crystallized in the form of needles and the major product (**4b**) formed as rhombohedral prisms; needles of **4a** were cut for the X-ray crystallographic analysis. Combined yield 42%. M.p.: **4a**; 158-160 °C; **4b**; 169-170 °C. Found: C, 33.45; H, 2.32; N, 6.07%. Calc. for $C_{26}H_{24}Cl_4Hg_2N_4$: C,33.36; H, 2.59; N, 5.99%. Λ_m (CH_3CN): 3 $\Omega^{-1}cm^2mol^{-1}$. IR (cm^{-1}): 1639 ν_{asym}(C(H)=N); 1593, 1485, 1440 ν(C=N)py. The IR spectra of **4a** and **4b** were

indistinguishable. ^{1}H-NMR (DMSO-d_6): δ8.87 [d, 1H, H-3′], 8.73 [s, 1H, H-7], 8.13 [m, 2H, H-5′,6′], 7.71 [dd, 1H, H-4′], 7.23 [m, 3H, H-,3,5,6], 7.06 [t, 1H, H-4], 2.41 [s, 3H, CH_3] ppm.

Synthesis of $[HgCl_2L^3]_2$ (**5**). A similar synthetic procedure to that used for **1** was used except that aniline was replaced by *m*-toluidine, giving-yellow crystals from acetonitrile solution. Yield 42%. M.p. 172-174 °C. Found: C, 33.25; H, 2.52; N, 5.86%. Calc. for $C_{26}H_{24}Cl_4Hg_2N_4$: C,33.36; H, 2.59; N, 5.99%. Λ_m (CH_3CN): 4 $\Omega^{-1}cm^2mol^{-1}$. IR (cm^{-1}): 1638 ν_{asym}(C(H)=N); 1593, 1487, 1434 ν(C=N)py. ^{1}H-NMR (DMSO-d_6): δ 8.91 [s, 1H, H-7], 8.87 [d, 1H, H-3′], 8.03 [m, 2H, H-5′,6′], 7.66 [t, 1H, H-4′], 7.28 [m, 3H, H-2,5,6], 7.10 [d, 1H, H-4], 2.32 [s, 3H, CH_3] ppm.

Synthesis of $[HgCl_2L^4]_2$ (**6**). A similar synthetic procedure to that used for **1** was used except that aniline was replaced by *p*-toluidine, giving pale-yellow crystals. Yield 43%. M.p. 230-232 °C. Found: C, 33.50; H, 2.66; N, 5.80%. Calc. for $C_{26}H_{24}Cl_4Hg_2N_4$: C, 33.36; H, 2.59; N, 5.99%. Λ_m (CH_3CN): 5 $\Omega^{-1}cm^2mol^{-1}$. IR (cm^{-1}): 1639 ν_{asym}(C(H)=N); 1593, 1467, 1434 ν(C=N)py. ^{1}H-NMR (DMSO-d_6): δ 8.94 [s, 1H, H-7], 8.86 [d, 1H, H-3′], 8.12 [d, 1H, H-6′], 8.02 [dd, 1H, H-5′], 7.73 [dd, 1H, H-4′], 7.05 [d, 2H, H-3,5], 7.30 [d, 2H, H-2,6], 2.41 [s, 3H, CH_3] ppm.

Synthesis of $[HgBr_2L^4]_2$ (**7**). A similar synthetic procedure to that used for **1** was used except that $HgCl_2$ and aniline were replaced by $HgBr_2$ and *p*-toluidine, respectively, giving pale-yellow crystals. Yield 53%. M.p. 206-208 °C. Found: C, 28.00; H, 2.22; N, 5.17%. Calc. for $C_{13}H_{12}Br_2HgN_2$: C, 28.03; H, 2.17; N, 5.03%. Λ_m (CH_3CN): 3 $\Omega^{-1}cm^2mol^{-1}$. IR (cm^{-1}): 1639 ν_{asym}(C(H)=N); 1593, 1480, 1447 ν(C=N)py. ^{1}H-NMR (DMSO-d_6): δ 8.87 [s, 1H, H-7], 8.71 [d,

1H, H-3′], 8.05 [d, 1H, H-6′], 7.91 [dd, 1H, H-5′], 7.66 [dd, 1H, H-4′], 7.45 [d, 2H, H-3,5], 7.19 [d, 2H, H-2,6], 2.33 [s, 3H, CH_3] ppm.

Synthesis of $[HgI_2L^4]_2$ (8). A similar synthetic procedure to that used for **7** was used except that $HgBr_2$ was replaced by HgI_2, giving pale-yellow crystals. Yield 59%. M.p. 194-196 °C. Found: C, 24.15; H, 2.02; N, 4.18%. Calc. for $C_{13}H_{12}HgI_2N_2$: C, 23.98; H, 1.86; N, 4.31%. Λ_m (CH_3CN): 5 $\Omega^{-1}cm^2mol^{-1}$. IR (cm^{-1}): 1639 ν_{asym}(C(H)=N); 1586, 1507, 1440 ν(C=N)py. ^{1}H-NMR (DMSO-d_6): δ 8.86 [s, 1H, H-7], 8.63 [d, 1H, H-3′], 8.04 [d, 1H, H-6′], 7.89 [dd, 1H, H-5′], 7.64 [dd, 1H, H-4′], 7.45 [d, 2H, H-3,5], 7.23 [d, 2H, H-2,6], 2.29 [s, 3H, CH_3] ppm.

Synthesis of $[Hg(NO_3)_2L^4]_n$ (9). The standard preparative method was slightly modified for this complex because of the low solubility of $Hg(NO_3)_2$ in ethanol. In this case, $Hg(NO_3)_2$(0.45 g, 1.40 mmol) was dissolved under heating in five drops of concentrated nitric acid and the resulting solution was diluted with 10 mL of water. This solution was added drop-wise to a previously prepared solution of pyridine-2-carboxaldehyde (0.15 g, 1.40 mmol) and *p*-toluidine (0.15 g, 1.40mmol) in ethanol (15 mL) which resulted in the immediate formation of a yellow precipitate. Stirring was continued for 3 h and then the mixture was filtered. The residue was washed thoroughly with water until the filtrate was pH neutral, then with methanol (3 x 5 mL) and dried *in vacuo*. The dried solid was dissolved in boiling acetonitrile (60 mL) and filtered while hot. The filtrate, upon cooling to room temperature afforded compound **9** in the form of a yellow crystalline material. Yield 0.47 g (58%). M.p. 220-221°C. Found: C, 30.15; H, 2.12; N, 10.80%. Calc. for $C_{13}H_{12}HgN_4O_6$: C, 29.96; H, 2.32; N, 10.76%. Λ_m (CH_3CN): 7 $\Omega^{-1}cm^2mol^{-1}$. IR (cm^{-1}) KBr: 1593 ν_{asym}(C(H)=N) + ν(C=N)py; 1527, 1381, 1321 ν(NO_3), Nujol: 1593

ν_{asym}(C(H)=N) + ν(C=N)py; 1527 $\nu_1(NO_3)$, 1334 $\nu_5(NO_3)$. ^{1}H-NMR (DMSO-d_6): δ 9.09 [s, 1H, H-7], 8.74 [d, 1H, H-3′], 8.10 [m, 2H, H-5′,6′], 7.77 [dd, 1H, H-4′], 7.07 [m, 4H, H-2,3,5,6], 2.19 [s, 3H, CH_3] ppm.

Synthesis of $\{[Hg(N_3)_2L^4]_2\}_n$ (10). To a solution of pyridine-2-carboxaldehyde (0.15 g,1.40 mmol) in ethanol (5 mL) was added a solution of *p*-toluidine (0.15g, 1.40 mmol) in ethanol (10 mL). The mixture was stirred at ambient temperature for 30 min. and was added drop-wise to a stirred methanolic solution containing $Hg(N_3)_2$ (prepared *in situ* from the reaction of $Hg(OAc)_2$ (0.45 g, 1.40 mmol) in 20 mL methanol with an excess of NaN_3 (0.36 g, 5.48 mmol) in 30 mL methanol) which resulted in the immediate formation of a yellow precipitate. The stirring was continued for 3 h and then the mixture was filtered. The residue was washed thoroughly with water, then with methanol (3 x 5 mL) and dried *in vacuo*. The dried solid was dissolved in boiling acetonitrile (60 mL) and filtered while hot. The filtrate, upon cooling to room temperature afforded yellow crystalline material. Yield 0.26 g (32%). M.p. 188-190 °C. Found: C, 32.66; H, 2.72; N, 23.42%. Calc. for $C_{26}H_{24}Hg_2N_{16}$: C, 32.45; H, 2.52; N, 23.30 %. Λ_m (CH_3CN): 3 $\Omega^{-1}cm^2mol^{-1}$. IR (cm^{-1}): 1639 ν_{asym}(C(H)=N); 1600; 1475, 1447 ν(C=N)py; 2037 $\nu_{as}(N_3)$. ^{1}H-NMR (DMSO-d_6): δ 8.70 [d, 1H, H-3′], 8.66 [s, 1H, H-7], 8.00 [dd, 1H, H-5′], 7.88 [d, 1H, H-6′], 7.44 [dd, 1H, H-4′], 7.21 [d, 2H, H-3,5], 7.15 [d, 2H, H-2,6], 2.30 [s, 3H, CH_3] ppm. *Caution: While no incident occurred while using azide during preparation and isolation, care in handling azides must be exercised owing to their potentially explosive nature.*

Quantum chemical calculations

Quantum chemical calculations were carried out on the ligands (L^1-L^4) in order to derive their structural parameters since the ligands could not be isolated in a pure crystalline form and characterized crystallographically. Previously, crystals of (*E*)-N-(pyridin-2-ylmethylidene)aniline (L^1) were obtained by sublimation and its crystal structure was reported;[51] however, the structure suffers from whole molecule disorder (see discussion). In view of unavailability of the pure ligands, the assignment of diagnostically important experimental infrared bands due to ν(C(H)=N) and ν(C=N)py was also difficult. To resolve these issues, the geometries of the ligands (L^1-L^4) were optimized using the B3LYP level of theory and the B3LYP/6-31G(*d*,*p*) basis set.[52] Harmonic frequency calculations were performed at all stationary points to characterize their nature and to ensure that the optimized structure corresponded with a global minimum. A similar method of calculation was successfully applied in the structural and spectroscopic characterization of a series of 2-hydroxy-5-[(*E*)-(aryldiazenyl)]benzaldehydes and 4-[((*E*)-1-{2-hydroxy-5-[(*E*)-2-(aryl)-1-diazenyl]phenyl}methylidene)amino]benzoic acid ligands.[53] A representative optimized structure, *e.g.* L^2, is shown in Fig. 1 while the other three molecules are given as ESI Figs S1-S3. The optimized geometric parameters for L^1-L^4 are listed in ESI Table S1. The experimental IR frequencies involve anharmonic terms whereas the calculated frequencies are derived from a harmonic oscillator model. This difference can be corrected by scaling the calculated values by a factor of 0.9623.[53,54] This information was utilized to interpret and assign the experimental infrared data for **1**-**10**.

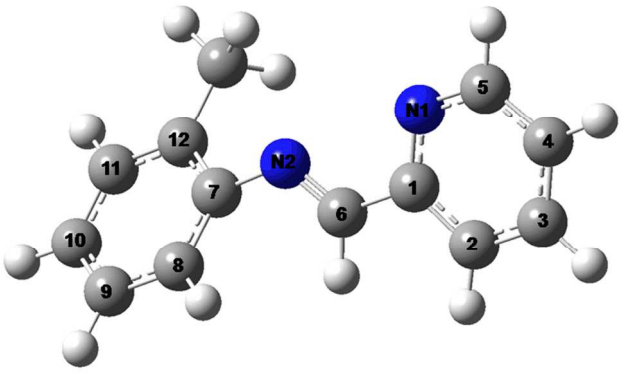

Fig. 1 A view of the geometry optimized structure of L^2.

X-ray crystallography

Crystals of compounds **2-10** suitable for X-ray crystal-structure determination were obtained by slow evaporation of acetonitrile solutions of the respective compounds at room temperature. In the case of compound **4**, the crystalline sample contained crystals of different shapes and full crystal structure determinations were conducted on each crystal form revealing two polymorphs. The measurements for **7-9** were made at low temperature on a Nonius KappaCCD diffractometer[55] with graphite-monochromated Mo Kα radiation (λ = 0.71073 Å) and an Oxford Cryosystems Cryostream 700 cooler. The data for **2, 3** and **10** were recorded on an Agilent Technologies Super Nova area-detector diffractometer[56] using Mo Kα radiation from a micro-focus X-ray source and an Oxford Instruments Cryojet XL cooler, and data for **4-6** were recorded on a Bruker-APEX diffractometer equipped with a CCD area detector and Mo Kα radiation. Data reduction was performed using HKL Denzo and Scalepack[57] for **7-9**, with CrysAlisPro[56] for **2**, **3** and **10**, and with SAINT[58] for **4-6**. An empirical absorption correction based on the multi-scan method[59] was applied for **4-9** while an analytical absorption correction[60] was applied for each of **2**, **3** and **10**. The structures of **7-9** were solved by heavy-atom Patterson methods[61] which

revealed the position of the Hg, Br and I atoms in their respective compounds. All remaining non-hydrogen atoms were located in a Fourier expansion of the Patterson solution, which was performed by *DIRDIF94*.[62] The structures of **2**, **4**-**6** and **10** were solved by direct methods using *SHELXS97*,[63] which revealed the positions of all non-hydrogen atoms while the structure of **3** was solved by direct methods using *SIR92*.[64] The non-hydrogen atoms in each structure were refined anisotropically. All of the H-atoms were placed in geometrically calculated positions and refined by using a riding model where each H-atom was assigned an isotropic displacement parameter with a value equal to $1.2U_{eq}$ of its parent atom ($1.5U_{eq}$ for methyl-H). The refinement of each structure was carried out on F^2 by using full-matrix least-squares procedures, which minimized the function $\Sigma w(F_o^2–F_c^2)^2$. For **3** and **9**, corrections for secondary extinction were applied and five and two reflections, respectively, were omitted owing to poor agreement. The absolute structure parameter of 0.259(7) for **7** indicated that the crystal investigated was an inversion twin. As is not uncommon for heavy atom structures, several data sets presented relatively large residual electron density peaks. Usually, these were located near the mercury atom, but in the cases of **7**, **9** and **10**, these were located in chemically meaningless positions. A comment on the large residual electron density peak in **2** is appropriate owing to its great size, *i.e*. 9.55 eÅ^{-3}. The minimum electron density peak was -1.36 eÅ^{-3} and the next highest peak was 1.00 eÅ^{-3}. The large residual peak was located 1.08 Å from the Hg atom and attempts were made to resolve its aetiology. The applied absorption corrected was based on face-indexing but when an empirical absorption correction was applied, the residual persisted. Similarly, the peak and pseudo-symmetry equivalent remained when the refinement was performed in the *P*1 space group; no evidence for twinning was found. While the residual may be indicative of disorder, no evidence of disorder was found in other parts of the molecule. The largest residual electron

density peak for **3** was also a little high at 5.32 eÅ^{-3}. The peak is within 0.93 Å of the Hg atom and the next highest peak was 0.88 eÅ^{-3}. Again, an absorption corrected based on face-indexing was applied. Other absorption correction trials did not reduce the peak and there was no evidence for twinning or disorder in the structure. The *SHELXL97* program[63] was used for the calculations of **2**, **3**, and **7**-**10**, while refinement and data output of **4**-**6** were carried out with the SHELXTL-NT program package.[65] The data collection and refinement parameters are given in Table 1, and views of the molecular structures are shown in Figs 4-8.

Results and discussion

Synthesis

In convenient one-pot reactions, a systematic series of ten complexes with the general stoichiometry HgX_2L has been prepared, where X is chloride, bromide, iodide, nitrate or azide, and L is a variously methyl-substituted Schiff base ligand, (*E*)-*N*-(pyridin-2-ylmethylidene)arylamine. In alcohol, one equivalent of HgX_2 reacts rapidly with one equivalent of L (generated *in situ* from pyridine-2-carboxaldehyde and a substituted aniline) to give a yellow precipitate which proved to be mercury complexes of the formula HgX_2L (**3**, **8**), $[HgX_2L]_2$ (**1**, **2**, **4**-**7**) and $[HgX_2L]_n$ (**10**), see Chart 1. Recently, the X-ray crystal structure for compound **1** was reported, but no spectroscopic properties were documented.[48] These are therefore included herein for comparative purposes. The synthesis of polymeric $[Hg(NO_3)_2L]_n$ (**9**) was conducted in an aqueous ethanol medium owing to the poor solubility of the mercury precursor in absolute ethanol. All mercury complexes are insoluble in the reaction medium, but can be recrystallized using a large volume of acetonitrile to provide crystals suitable for X-ray diffraction studies. The results of the crystal structure determinations of **2**-**10** are consistent with

the chemical and spectroscopic analyses, giving clear evidence of the formation of 1:1 adducts between the bidentate N-donors and the corresponding HgX_2. Complexes **2**-**10** are all air-stable and behave as non-electrolytes in acetonitrile solution.

Table 1 Crystal data and refinement details for **2-10**

	2	**3**	**4a**	**4b**
Empirical formula	$C_{24}H_{20}Br_4Hg_2N_4$	$C_{12}H_{10}HgI_2N_2$	$C_{26}H_{24}Cl_4Hg_2N_4$	$C_{26}H_{24}Cl_4Hg_2N_4$
Formula weight	1085.06	636.53	935.47	935.47
Crystal size (mm)	0.05 × 0.10 × 0.10	0.10 × 0.15 × 0.15	0.15 × 0.16 × 0.20	0.15 × 0.21 × 0.22
Crystal morphology	Prism	Prism	Prism	Prism
Temperature (K)	160(1)	160(1)	293(2)	293(2)
Crystal system	Triclinic	Monoclinic	Triclinic	Triclinic
Space group	$P\bar{1}$	$P2_1/n$	$P\bar{1}$	$P\bar{1}$
a (Å)	8.03383(16)	12.68311(19)	8.2038(11)	12.0247(16)
b (Å)	8.9441(2)	7.13335(10)	13.8179(19)	14.3877(19)
c (Å)	10.0091(3)	15.9101(2)	14.4494(19)	17.542(2)
α(°)	106.595(3)	90	115.149(2)	78.370(2)
β(°)	100.732(2)	90.8269(13)	99.505(2)	83.453(2)
γ(°)	99.5612(19)	90	100.406(2)	78.383(2)
V (Å^3)	658.57(3)	1439.28(4)	1403.5(3)	2903.2(7)
Z	1	4	2	4
D_x (g cm^{-3})	2.736	2.938	2.214	2.140

μ (mm^{-1})	17.694	14.964	11.330	10.954
Transmission factors (min, max)	0.145, 0.358	0.168, 0.336	0.210, 0.281	0.197, 0.290
θ range(°)	2.2–32.6	3.1–32.4	1.7–25.0	1.2 –25.0
Reflections measured	20442	22859	13697	28274
Independent reflections; R_{int}	4394; 0.033	4851; 0.035	4934; 0.056	10210; 0.057
Reflections with $I > 2\sigma(I)$	4057	4367	3716	5153
Number of parameters	154	155	327	653
$R(F)$ [$I > 2\sigma(I)$ reflns]	0.038	0.027	0.040	0.038
$wR(F^2)$ (all data)	0.100	0.066	0.133	0.057
GOF(F^2)	1.07	1.05	1.04	0.99
$\Delta\rho_{max, min}$ (e Å^{-3})	9.55, -1.36	5.32, -1.49	1.38, -1.08	1.19, -0.81

5	6	7	8	9	10
$C_{26}H_{24}Cl_4Hg_2N_4$	$C_{26}H_{24}Cl_4Hg_2N_4$	$C_{26}H_{24}Br_4Hg_2N_4$	$C_{13}H_{12}HgI_2N_2$	$C_{13}H_{12}HgN_4O_6$	$C_{26}H_{24}Hg_2N_{16}$
935.47	935.47	1113.32	650.64	520.86	961.79
0.23 × 0.34 × 0.46	0.27 × 0.29 × 0.34	0.10 × 0.12 × 0.18	0.22 × 0.25 × 0.25	0.10 × 0.13 × 0.30	0.08 × 0.13 × 0.20
Prism	Prism	Prism	Prism	Prism	Tablet
293(2)	293(2)	160(1)	160(1)	160(1)	160(1)
Monoclinic	Monoclinic	Monoclinic	Triclinic	Monoclinic	Triclinic
$P2_1/c$	$P2_1/n$	$P2_1$	$P\bar{1}$	$P2_1/c$	$P\bar{1}$
7.7944(9)	7.5731(19)	8.2201(1)	7.7545(1)	10.6101(2)	6.6753(2)
8.4673(10)	15.346(4)	17.5934(3)	9.9076(2)	14.2146(2)	10.3614(3)
21.336(2)	12.503(3)	10.0430(2)	10.9202(2)	10.3608(2)	11.5961(4)
90	90	90	76.889(1)	90	71.528(3)
95.221(2)	97.653(4)	104.6895(9)	83.930(1)	97.2161(11)	73.693(3)
90	90	90	76.652(1)	90	78.321(3)
1402.3(3)	1440.2(6)	1404.94(4)	793.78(2)	1550.22(5)	724.43(4)
2	2	2	2	4	1
2.216	2.157	2.632	2.722	2.232	2.205

11.339	11.041	16.626	13.570	9.968	10.633
0.078, 0.180	0.117, 0.155	0.152, 0.213	0.033, 0.072	0.145, 0.388	0.280, 0.721
2.6– 25.0	2.1–25.0	2.1–30.0	1.9–27.5	25–30.0	2.4 – 30.5
12935	13356	41875	17262	42486	18011
2465; 0.054	2528; 0.068	8003; 0.054	3607; 0.075	4503; 0.080	4055; 0.033
2096	1885	7309	3330	3755	3767
164	164	328	164	219	200
0.029	0.041	0.032	0.040	0.031	0.020
0.063	0.076	0.073	0.105	0.074	0.042
0.96	1.06	1.04	1.07	1.04	1.07
1.07, -1.15	0.72, -1.04	2.36, -2.00	1.23, -4.19	2.04, -1.60	1.02, -0.75

Geometry optimized structures of L^1-L^4

Although the crystal structure of (*E*)-*N*-(pyridin-2-ylmethylidene)aniline(L^1) has been reported,[51] the geometric parameters could not be used with confidence owing to whole molecule disorder. As anticipated, most of the geometric parameters in the calculated structures of L^1-L^4 (ESI Table S1) are found to be insensitive to the nature and position of the substituents. However, the substituents can have a profound effect on the planarity of the molecule. The basic structural framework of each of L^1-L^4contains one pyridine ring and one aryl ring connected through the C(H)=N linkage, and these are planar in the optimized structures of L^1, L^3 and L^4. However, L^2 is non-planar as seen in the C6-N2-C7-C8 torsion angle of 41.3°, an observation correlated with steric pressure should a planar arrangement be adopted. Molecules L^1-L^4 exist in the *trans*-isomeric form, as observed by Wiebcke *et al*.[51] The stretching vibrational frequencies due to C(H)=N (1640 cm^{-1}) and ν(C=N)py (1575 cm^{-1}) are found to be almost unchanged in L^1-L^4 and this assignment was used to diagnose the said bands in the experimental infrared spectra of complexes **1**-**10**. Finally, the Mulliken charges were calculated based on the optimised structures. This showed that the charge distribution on the N1 and N2 atoms of L^1 (-0.4562 and -0.4317) and L^3 (-0.4564 and -0.4324) were virtually identical and less than those calculated for L^2 (-0.4582 and -0.4367) and L^4 (-0.4567 and -0.4349).

IR, NMR, UV-Vis and fluorescence spectroscopy

The infrared spectra of complexes **1**-**10** are very similar and the IR assignments of selected diagnostic bands are given in the Experimental section. The complexes display a moderately intense IR band in the region 1630-1650 cm^{-1}, which is assigned to the ν_{asym}(C(H)=N) stretch of the coordinated Schiff base ligands.[66] In addition, well resolved sharp bands of variable intensity

observed in the regions 1600-1580, 1490-1475 and 1450-1435 cm^{-1} are assigned to the coordinated pyridine ring.[66-68] Complexes **9** and **10** deserve specific mention. The cited nitrate frequencies in **9** are medium-dependent. Using a KBr matrix, the IR spectrum showed a very strong band at approximately 1381 cm^{-1} which is indicative of the simultaneous presence of ionic and coordinated nitrates;[67] it is noted that pressing a KBr pellet can also influence the nitrate coordination which has been fully discussed in the literature.[69] In addition, the solid-state spectrum of **9** displayed bands at 1527 and 1321 cm^{-1}, which are indicative of bidentate chelating nitrate groups. The assumption of bidentate chelating nitrate groups[67] was further established from the nitrate vibrations observed in the Nujol mull spectrum of **9**, since the separation of the two bands ν_1 and ν_5 is approximately 200 cm^{-1} ($\nu_1(NO_3)$ 1527 cm^{-1}, $\nu_5(NO_3)$ 1334 cm^{-1}).[70] The bidentate coordination mode of the nitrate groups was subsequently confirmed by the X-ray crystal structure determination (see below). On the other hand, an important observation for the IR spectrum of **10** is the presence of a very strong band at 2037 cm^{-1} corresponding to $\nu_{asym}(N_3)$; the bridging nature of N_3^- is revealed by weak doublet splitting.[71,72]

The ^1H NMR spectra recorded in DMSO-d_6 solution displayed the expected signals,[73,74] and, therefore, revealed the presence of the ligand skeleton in the respective complexes. Coupling constants could not be established with certainty owing to the broad unresolved nature of the signals. The effect of coordination to mercury(II) upon the ^1H NMR chemical shifts could not be judged in the absence of the NMR data for the ligands, which could only be prepared *in situ* (see Experimental).

Table 2 summarizes the solution UV-Vis and fluorescence properties of complexes **1-10**; spectra remained unchanged over a period of 25 days. The absorption spectra of all complexes were recorded in the range 300-450 nm in acetonitrile solutions at concentrations of ~10^{-5} M.

The electronic spectra exhibit a coalescence absorption in the range of 325 to 360 nm (Fig. 2) and the origin of the band could not be assigned unambiguously due to the non-availability of data for the free ligands. Nevertheless, the absorption is possibly a result of overlap of intramolecular charge transfer transitions ($\varepsilon \sim 10^4$) with a weak band due to MLCT transition from Hg(II) $\rightarrow \pi^*$ (ligand), as observed for the cognate systems.[75,76]

The steady-state fluorescence studies have been employed as independent evidence of complexation. In acetonitrile solution, the complexes have broad emission bands at λ_{max} = 410 nm along with a shoulder at ~430 nm within the wavelength range of 390-550 nm, when they are excited at their respective absorption maxima (Fig. 3), indicating that the transitions are charge transfer in nature. In general, the complexes show very low fluorescent quantum yields, which can be attributed to the heavy atom effect.[77,78] The Hg^{2+} cation and chloride anions can quench the fluorescence and result in efficient luminescence decay. However, complexes **3**, **8** and **10** exhibit a very weak emission yield, which is about one order of magnitude lower than for the remaining complexes. It can be presumed that the significantly weakened emission intensities for **3** and **8**, when compared with the related analogues **1**-**2** and **6**-**7**, respectively, can be attributed to the competitive quenching effect of the iodide ions.[79] The difference in the intensity of the emission results from the variation of the coordinated anions to mercury(II), and indicates that the anions strongly affect the fluorescence emission features.[25,80]

Table 2 Photophysical data for complexes **1-10** recorded in acetonitrile solution

Complexes	Electronic absorption data	Photoluminescence data	
	λ_{max} (nm); (ε[M^{-1}])	λ_{em}(nm)[a]	ϕ_F
1	336 (12698)	409,431	0.21
2	338 (25190)	410, 432	0.19
3	331 (33717)	408, 434	0.08
4	356 (16258)	409, 437	0.27
5	338 (45680)	409, 430	0.19
6	348 (10781)	413, 429	0.16
7	341 (13367)	410, 432	0.20
8	340 (32679)	411, 433	0.02
9	360 (29458)	410, 434	0.39
10	325 (31701)	411, 432	0.03

[a]The low energy wavelength emission appears as a shoulder in all cases.

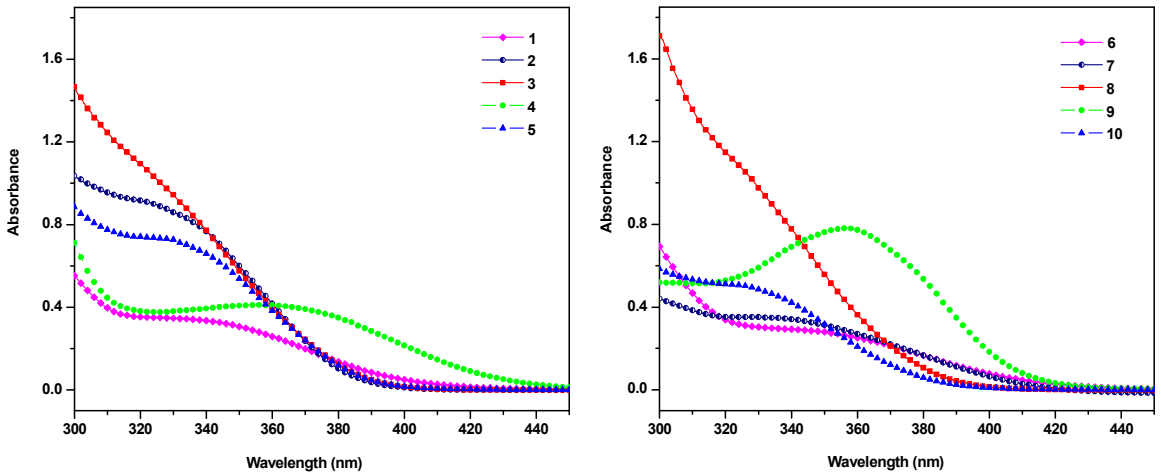

Fig. 2 UV–Vis spectra of complexes **1-10** in acetonitrile (concentration ~10^{-5} M).

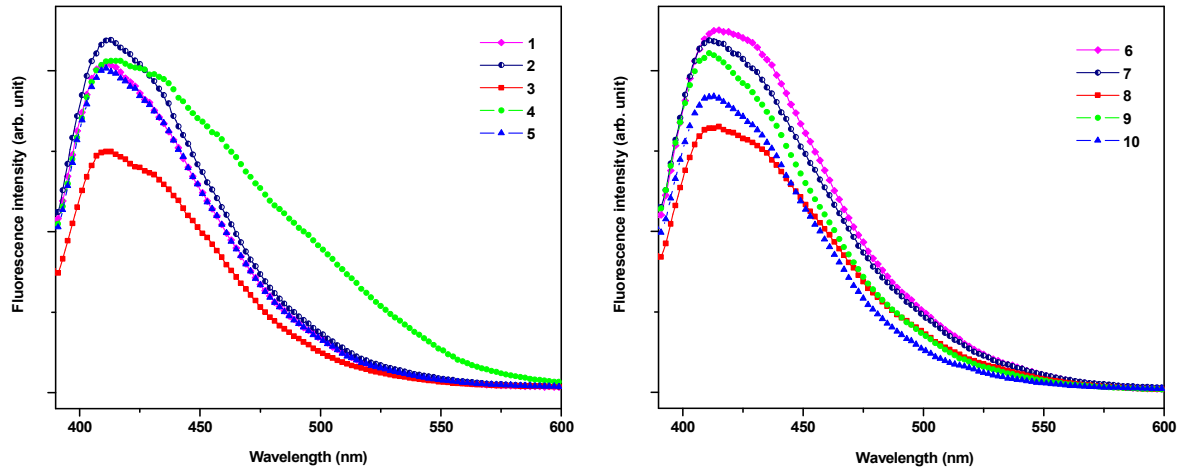

Fig. 3 Fluorescence spectra of complexes **1-10** in acetonitrile (concentration ~10^{-5} M) obtained by excitation at the respective absorption maxima.

Molecular structures

The crystal and molecular structures of **2-10** have been determined in the present study and reveal a variety of structural motifs; the structure of **1** is available in the literature.[48] Herein, the

molecular structures will be described in order of increasing nuclearity. Selected geometric parameters are collected in Tables 3 and 4.

Mononuclear species are found for the diiodido complexes [HgI_2L^1] (**3**) and [HgI_2L^4] (**8**), Fig. 4. In each case, the mercury atom is tetrahedrally coordinated by two iodine atoms and the nitrogen atoms derived from the chelating ligand. The persistent trend in the series of structures reported herein is the presence of chelating (*E*)-N-(pyridin-2-ylmethylidene)arylamine ligands and the observation that the Hg–N(pyridyl) bond length is consistently shorter than the Hg–N(imino) bond length (Δ(Hg–N) = 0.12 to 0.26 Å, except for **8** where it is only 0.03 Å). Across the series of structures, the parameters about the N(2)=C(6) bond do not differ experimentally (Tables 3 and 4), are comparable with the parameters derived from the geometry optimised structures (ESI Table S1), and are, therefore, not discussed further. The five-membered chelate ring in **3** is planar with the root-mean-square (r.m.s.) deviation for the fitted atoms being 0.026 Å, and indeed the overall molecule of L^1 is planar as seen in the dihedral angle of 3.19(17)º formed between the pyridyl and phenyl rings. In this structure and across the series, the Hg-N-C bond angles follow the same trends with the exo-chelate ring angles being approximately 8º (N1) and 12º (N2) wider than the endo-chelate ring angles (Tables 3 and 4).

A similar coordination geometry pertains in the structure of **8**, the r.m.s. deviation of the chelate ring and dihedral angle between the six-membered rings being 0.074 Å and 4.5(3)º, respectively. Fig. S4 shows an overlay diagram of molecules **3** and inverted **8** highlighting the similarity in the mode of coordination of the bidentate ligands. However, the distortions from the ideal tetrahedral geometry are larger in **3** (range of tetrahedral angles = 70.47(11) to 124.84(8)º) than in **8** (69.73(18) to 114.55(12)º). The more symmetrical arrangement in **8** correlates with a more symmetric mode of coordination of L^4, and is seen in the small difference of the Hg–N

bond distances, Δ(Hg–N), of 0.04 Å. This compares with Δ(Hg–N) = 0.12 Å for **3** and correlates with the increase in basicity of the imino-N2 atom in L^4 owing to the electron donating nature of the methyl group.

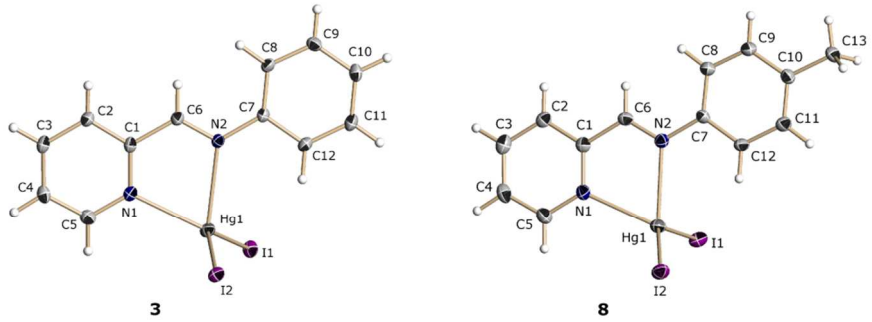

Fig. 4 Perspective views of the monomers found in the crystal structures of compounds $[HgI_2L^1]$ (**3**) and $[HgI_2L^4]$ (**8**). Displacement ellipsoids are drawn at the 30% probability level and H atoms are shown as small spheres of arbitrary radii.

It was also possible to characterize crystallographically the dibromido analogues of **3** and **8**, *i.e.* $[HgBr_2L^1]_2$ (**2**) and $[HgBr_2L^4]_2$ (**7**), for which notable structural changes were observed, Fig. 5. Molecules of **2** are formed by self-association of the mononuclear entity over a centre of inversion *via* secondary Hg···Br interactions. The Hg–Br1 bond length of 2.6299(6) Å is significantly longer than the terminal Hg–Br2 bond (2.5203(6) Å), consistent with the participation of the Br1 atom in the bridge to the second Hg atom of the binuclear molecule. The Hg_2Br_2 cycle is not symmetric as the bridging Hg···Br distance is 3.0140(6) Å, a value significantly less than the sum of the van der Waals radii of mercury and bromine of 3.40 Å.[81] The resulting Br_3N_2 donor set defines a coordination geometry intermediate between square pyramidal and trigonal bipyramidal as quantified by the value of $\tau = 0.32$ which compares to the

τ values of 0.0 and 1.0 for ideal square pyramidal and trigonal bipyramidal geometries, respectively.[82]

As for **2**, the molecules in **7** self-associate but this time through a non-crystallographic centre of inversion. The two independent entities, containing Hg1 or Hg21, comprise the asymmetric unit with the inverted form of the Hg21-containing molecule virtually superimposable upon that with Hg1 (ESI Figure S5). This similarity is reflected in the r.m.s. deviation of bond lengths and angles of 0.014 Å and 1.49º, respectively.[83] A dramatic influence exerted by the methyl substituent of L^4 in the self-association of **7** is evident from the bridging Hg···Br distances in **7**, which are significantly longer than in **2**, *i.e*. 3.4749(8) and 3.6344(8) Å, and larger than the sum of their van der Waal radii (3.40 Å).[81] The more covalent character of the Hg–Br bond can be correlated with the better coordinating ability of the L^4 ligand compared with L^1, as reflected in the shorter Hg–N bond lengths, Table 3, and as discussed above for the structures of **3** and **8**.

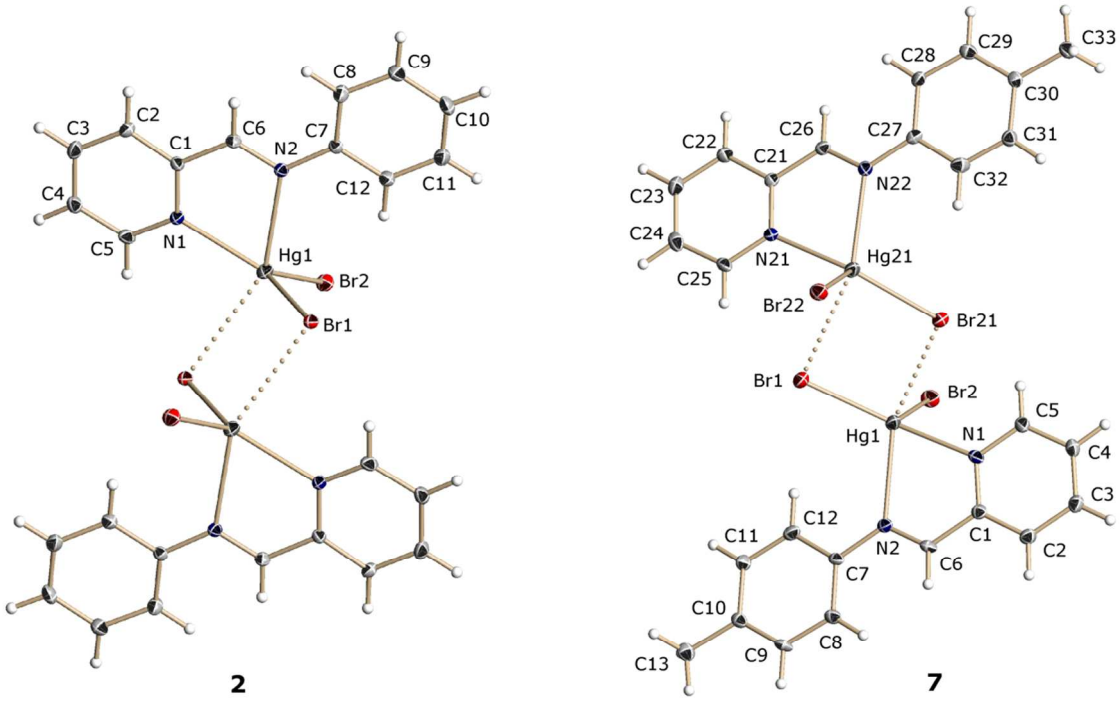

Fig. 5 Perspective views of the weakly associated dimers found in the crystal structures of $[HgBr_2L^1]_2$(**2**) and $[HgBr_2L^4]_2$(**7**). Displacement ellipsoids are drawn at the 30% probability level and H atoms are shown as small spheres of arbitrary radii.

Table 3 Selected bond lengths (Å) and angles (º) for **1-8** and **10**[a]

	1[b]	**2**	**3**	**4a**[b]	**4b**[b] **(molec. A)**	**4b**[b] **(molec. B)**	**5**	**6**	**7**[b]	**8**	**10**[c]
Hg1–N1	2.322(8)	2.327(4)	2.357(3)	2.256(7) 2.337(8)	2.362(6) 2.338(6)	2.347(6) 2.366(6)	2.276(4)	2.354(6)	2.288(6) 2.295(6)	2.404(5)	2.232(2)
Hg1–N2	2.497(7)	2.507(4)	2.478(3)	2.512(8) 2.499(8)	2.489(6) 2.507(6)	2.516(6) 2.503(6)	2.500(4)	2.490(6)	2.471(5) 2.467(5)	2.438(5)	2.496(3)
Hg1–X1	2.526(3)	2.6299(6)	2.6446(3)	2.474(3) 2.428(3)	2.411(2) 2.411(2)	2.416(2) 2.393(2)	2.4207(14)	2.423(2)	2.5010(7) 2.4994(7)	2.6698(5)	2.125(2)
Hg1–X1'	2.896(3)	3.0140(6)	-	3.026(3) 2.983(3)	3.155(2) 3.056(2)	3.169(2) 3.155(2)	2.9837(15)	3.011(2)	3.4749(8) 3.6344(8)	-	2.823(2)
Hg1–X2	2.396(3)	2.5203(6)	2.6964(3)	2.410(3) 2.382(3)	2.383(2) 2.389(2)	2.372(2) 2.383(2)	2.4376(13)	2.355(3)	2.5779(8) 2.5831(7)	2.6363(5)	2.468(2)
Hg1–X2'	-	-	-	-	-	-	-	-	-	-	2.579(2)
C1–C6	1.478(12)	1.475(7)	1.474(5)	1.459(14) 1.467(15)	1.455(9) 1.451(10)	1.473(9) 1.464(10)	1.473(7)	1.477(10)	1.477(9) 1.453(9)	1.471(9)	1.461(4)
N2–C6	1.270(12)	1.268(7)	1.276(5)	1.259(11) 1.248(12)	1.284(8) 1.275(8)	1.281(8) 1.277(8)	1.265(6)	1.258(9)	1.278(9) 1.283(8)	1.264(8)	1.274(3)
N2–C7	1.417(11)	1.419(7)	1.421(5)	1.444(12) 1.426(13)	1.413(8) 1.414(10)	1.441(8) 1.438(9)	1.429(6)	1.420(9)	1.434(8) 1.418(8)	1.418(7)	1.417(4)
N1–Hg1–N2	70.3(3)	70.44(15)	70.47(11)	70.8(3) 68.5(3)	69.3(2) 69.1(2)	69.6(2) 68.4(2)	71.22(14)	70.3(2)	71.13(18) 71.30(18)	69.73(18)	71.05(8)
N1–Hg1–X1	126.6(2)	126.56(11)	124.84(8)	127.7(2) 103.3(2)	111.21(16) 111.80(18)	104.84(16) 112.21(16)	143.12(11)	107.73(16)	144.52(13) 141.55(14)	104.46(13)	158.28(10)
N1–Hg1–X2	118.0(2)	118.84(11)	100.53(8)	123.3(2) 131.1(2)	117.00(16) 114.40(17)	121.84(16) 113.25(16)	105.99(11)	113.76(17)	96.39(13) 100.57(14)	114.29(14)	91.82(8)
N2–Hg1–X1	91.69(18)	91.40(10)	105.79(7)	108.17(19)	112.65(15)	114.50(15)	103.76(9)	94.10(15)	107.83(12)	101.71(12)	118.41(9)

				114.8(2)	114.97(16)	113.23(16)			108.38(12)		
N2–Hg1–X2	109.3(2)	109.66(11)	107.52(7)	93.63(19) 91.2(2)	92.82(15) 90.50(15)	94.54(14) 91.02(16)	112.40(9)	104.98(15)	111.26(12) 113.72(12)	114.55(12)	80.13(7)
N1–Hg1–X1'	84.9(2)	84.90(11)	-	87.3(2) 87.2(2)	85.76(17) 84.46(18)	84.59(17) 84.35(17)	83.01(10)	87.35(16)	74.98(13) 74.97(13)	-	83.85(7)
N2–Hg1–X1'	144.45(19)	146.02(11)	-	158.04(18) 150.6(2)	153.83(16) 151.02(17)	151.28(16) 151.52(17)	143.45(10)	156.50(16)	130.20(13) 129.66(12)	-	119.61(8)
N1–Hg1–X2'	-	-	-	-	-	-	-	-	- -	-	84.57(8)
N2–Hg1–X2'	-	-	-	-	-	-	-	-	-	-	146.87(8)
X1–Hg1–X2	115.35(10)	114.59(2)	130.455(11)	108.93(9) 125.56(10)	130.93(7) 132.77(7)	131.56(7) 133.76(7)	109.40(5)	138.07(11)	115.66(3) 113.36(3)	133.685(17)	108.70(9)
X1–Hg1–X1'	82.91(8)	84.768(17)	-	84.28(9) 86.02(9)	83.06(6) 85.24(6)	83.48(6) 84.14(6)	81.50(5)	85.66(7)	80.75(2) 77.54(2)	-	74.50(10)
X1–Hg1–X2'	-	-	-	-	-	-	-	-	-	-	92.44(9)
X2–Hg1–X1'	104.66(10)	102.542(19)	-	99.41(9) 92.67(11)	91.64(6) 89.79(6)	88.40(6) 92.22(7)	99.15(5)	90.34(7)	107.78(2) 108.31(2)	-	156.52(8)
X2–Hg1–X2'	-	-	-	-	-	-	-	-	-	-	78.57(8)
Hg1–X1–Hg1'	97.09(8)	95.232(17)	-	94.08(8) 93.96(8)	94.53(6) 97.10(7)	95.94(7) 96.04(7)	98.50(5)	94.34(7)	98.70(2) 102.94(2)	-	105.50(10)
Hg1–X2–Hg1'	-	-	-	-	-	-	-	-	-	-	101.43(8)
Hg1–N1–C1	116.7(6)	116.6(3)	116.2(3)	116.8(6) 118.2(7)	116.9(5) 118.0(6)	118.4(5) 118.4(6)	117.2(3)	116.5(5)	117.5(4) 116.6(4)	114.6(4)	118.24(18)
Hg1–N1–C5	124.3(7)	124.4(4)	124.7(3)	123.9(6) 123.6(7)	124.1(5) 125.4(6)	124.5(5) 123.6(5)	123.3(3)	124.9(5)	123.1(4) 123.0(5)	125.9(5)	121.81(18)

Hg1–N2–C6	112.6(6)	111.9(3)	112.7(3)	109.2(6) 112.8(7)	113.4(5) 110.2(6)	112.0(5) 112.4(6)	110.7(3)	112.6(5)	111.9(4) 111.3(4)	115.1(4)	110.31(18)
Hg1–N2–C7	125.8(6)	126.8(3)	125.5(2)	129.5(6) 121.7(6)	124.1(5) 123.3(5)	127.3(4) 123.8(5)	128.9(3)	125.6(5)	126.5(4) 126.8(4)	122.5(4)	125.40(18)

[a] Compounds **1**, **2**, **5** and **6** are dinuclear complexes in which the participating molecules are related by a crystallographic centre of inversion. Compounds **4a**, **4b** and **7** are also dinuclear complexes, but the participating molecules are crystallographically independent. In the case of compound **4b**, the asymmetric unit contains two such dimers (A and B). Analogous atom numbering schemes have been used in all cases. Therefore, for the sake of clarity, in column 1 only labels for one of the independent molecules are given. Primed atoms indicate the longer Hg···X bridging distance to the second unit of the dimer.

[b] Data taken from ref. 48.

[c] Compound **10** is a one-dimensional polymer with centrosymmetric double azide bridges between adjacent Hg-atoms. There are two symmetry-independent pairs of bridges. One contains atom N3 (X1) and its inversion-related counterpart, while the other involves N6 (X2) and its counterpart.

With the structure of $[HgCl_2L^1]_2$ (**1**) having being reported previously in the literature,[48] the complete series of $HgCl_2$ structures with L^{1-4} is available for comparison, Fig. 6 and Table 3. Compound $[HgCl_2L^2]_2$ (**4**) crystallizes in two polymorphic triclinic forms, which were deposited concomitantly from the same recrystallization and can be distinguished by their different crystal shapes: needles for the minor product (**4a**) and rhombohedral prisms for the major product (**4b**).

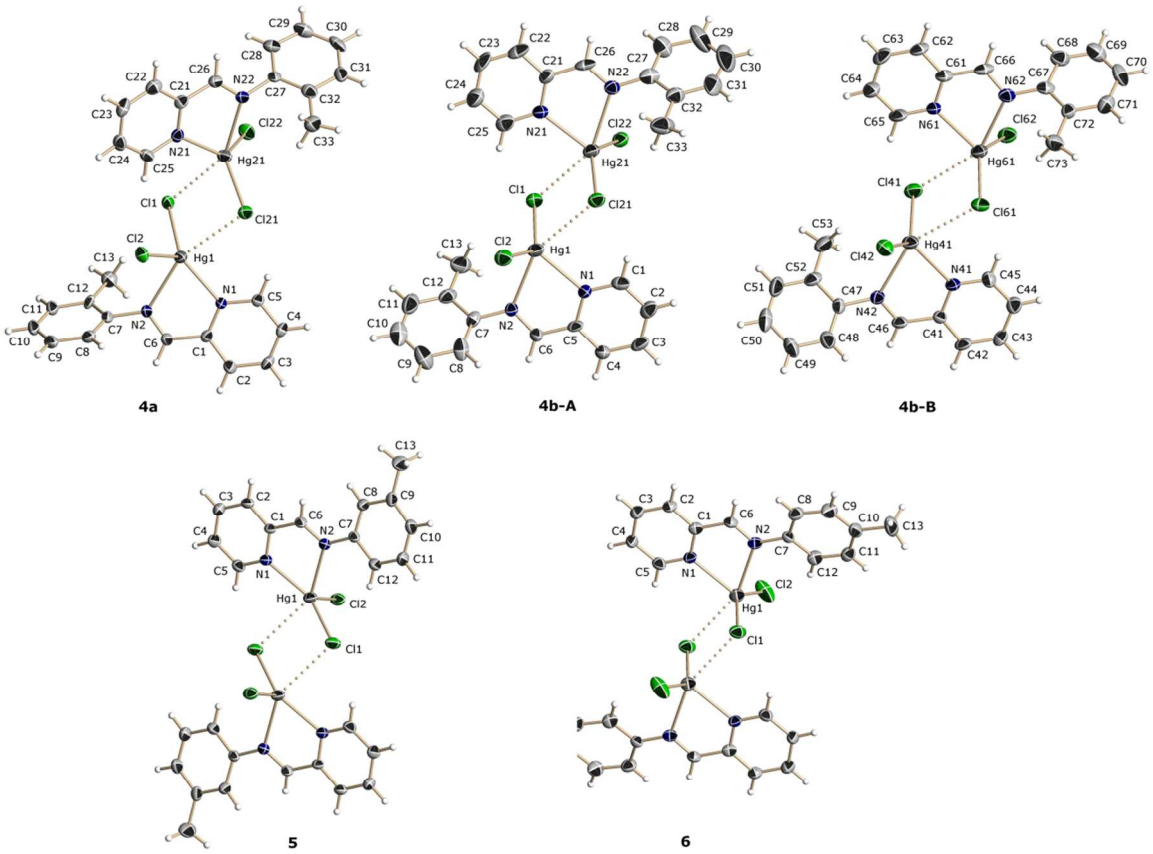

Fig. 6 Perspective views of the dimers found in the crystal structures of the polymorphic forms of $[HgCl_2L^2]_2$ (**4a** and **4b**), $[HgCl_2L^3]_2$ (**5**) and $[HgCl_2L^4]_2$ (**6**). Displacement ellipsoids are drawn at the 30% probability level and H atoms are shown as small spheres of arbitrary radii.

In **4a** and **4b**, two and four independent mononuclear entities comprise the asymmetric unit, respectively, with the dinuclear species arising from association *via* non-crystallographic

centres of inversion. It can be seen from the overlay diagram, Fig. 7, drawn with Qmol,[84] that while the pyridyl residues are virtually superimposable in the six independent molecules, differences appear in the dihedral angles formed between this and the tolyl residues (range = 40.9(4) to 70.4(5)º) and in the relative orientation of the chloride ligands. The higher calculated density in **4a** (2.214 g cm^{-3}) compared with that of **4b** (2.140 g cm^{-3}) is reflected in the higher packing index[83] for **4a** (0.670 *cf.* 0.648), and suggests that the needles of **4a** are thermodynamically more stable.

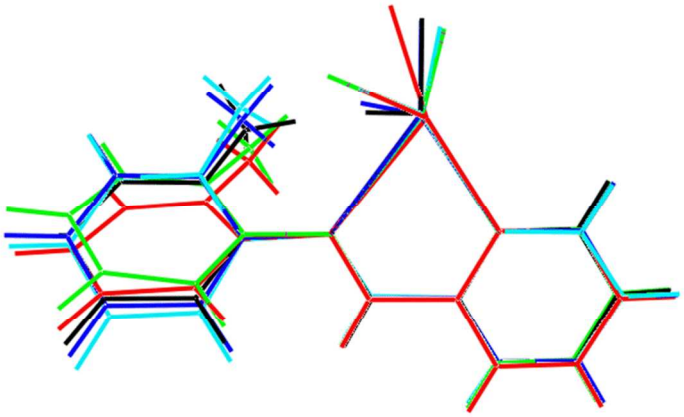

Fig. 7 Overlay diagram of $HgCl_2L^2$ molecules in polymorphic **4a** (the Hg1- and inverted Hg21-containing molecules are illustrated in red and green, respectively) and **4b** (the Hg1-, inverted Hg21-, Hg41 and inverted Hg61-containing molecules are illustrated in blue, pink, light-blue and black, respectively). The molecules have been aligned to make the five-membered chelate rings coincident.

In each of $[HgCl_2L^1]_2$ (**1**),[48] $[HgCl_2L^3]_2$ (**5**) and $[HgCl_2L^4]_2$ (**6**), the dinuclear molecule is generated by the application of a centre of inversion. The respective (*E*)-N-(pyridin-2-ylmethylidene)arylamine ligands in these structures are considerably less twisted than in the sterically congested complexes **4a** and **4b**, with the dihedral angle between the two rings in each of **1**, **5** and **6** being 11.7(6), 9.0(3) and 13.2(4)º, respectively.

The relatively large standard uncertainty values associated with the Hg–N bond lengths across the series of the $[HgCl_2L]_2$ structures preclude definitive conclusions about the relative coordinating abilities of L^{1-4} molecules, but this can be ascertained indirectly by consideration of the Hg–Cl bond lengths. Thus, the Hg–Cl1 and Hg···Cl1 bond lengths are systematically shorter and longer, respectively, in the structures involving the methyl-substituted ligands compared with those incorporating the unsubstituted ligand, Table 3. In terms of coordination geometry, the values of τ were generally around 0.30 for the mercury atoms in **1**, **4a** (Hg21), **4b** and **6** with exceptional values being found for the Hg1 atom in each of **4a** (0.50) and **5** (0.01).

Clear trends are evident from the structural data on the aforementioned HgX_2L species in that when X = I, no evidence for Hg···I bridges was found, but weak Hg···X bridges and clear pairing of mononuclear entities started to appear in structures with X = Br and were uniformly characterized in the structures with X = Cl. Also of interest was the observation that the coordinating ability of the (*E*)-N-(pyridin-2-ylmethylidene)arylamine molecules is significantly moderated by the presence of methyl substituents in the aryl rings and this in turn reduced the propensity of the Hg···X bridge formation.

Next, attention was directed to investigating structures with X = nitrate (**9**) and azide (**10**). In the structure of (**10**), containing the pseudo-halide ligand azide, the familiar centrosymmetric dimer is found, Fig. 8 and Table 4. Here, the bridge involves the terminal N6 atom and the difference in Hg–N bond lengths (0.27 Å) indicates a relatively symmetric bridge. The value of τ is 0.19 indicating a gap in the coordination geometry which is occupied by a weakly associated N3 atom (Hg–N = 2.823(2) Å *cf*. the sum of the van der Waals radii of Hg and N of 3.10[81]) that serves as a bridge to link the dimeric aggregates into a supramolecular chain along the *a*-axis, Fig. 8b.

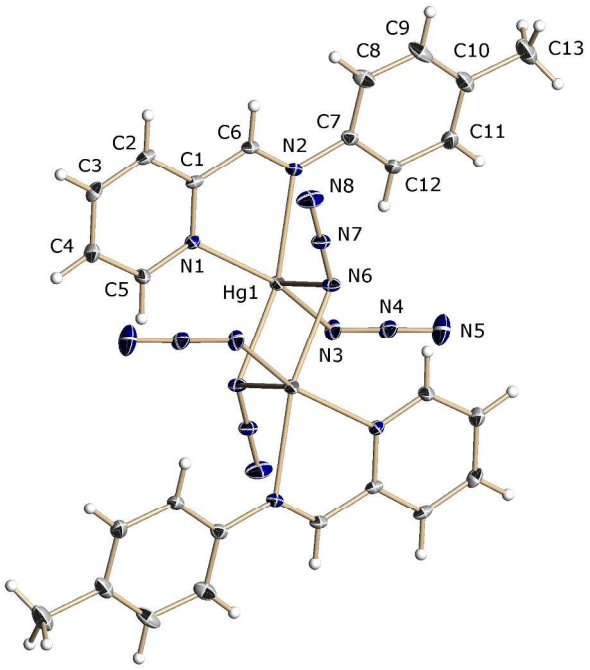

a)

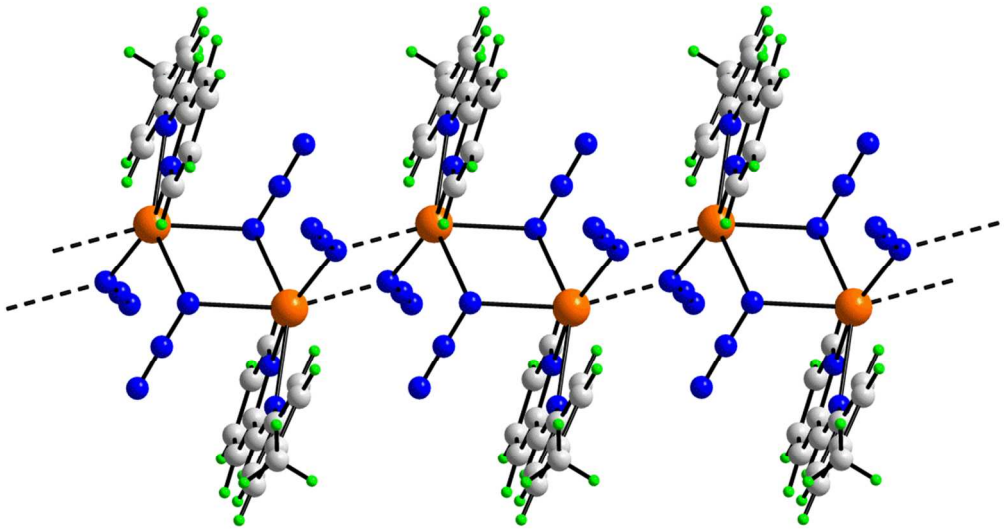

b)

Fig. 8 Perspective views of $[Hg(N_3)_2L^4]$: (a) two centrosymmetrically-related azide-bridged units, and (b) the $\{[Hg(N_3)_2L^4]_2\}_n$ extended chain found in the crystal structure of compound **10**.

Displacement ellipsoids for a) are drawn at the 30% probability level and H atoms are shown as small spheres of arbitrary radii.

The final structure to be described is that of the nitrate analogue of the foregoing series, $[Hg(NO_3)_2L^4]$ (**9**), which differs considerably in terms of coordination geometry and mode of association of anions. Within the asymmetric unit, Fig. 9a, the mercury atom is chelated by the (*E*)-N-(pyridin-2-ylmethylidene)arylamine and two nitrate ligands, one, containing the N3 atom, symmetrically and the other (with N4) asymmetrically, as reflected in the disparate Hg–O bond lengths and Hg–O–N bond angles in the latter, Table 5. The N3-nitrate forms an additional two interactions with a symmetry-related (glide operation) mercury atom and serves to link the molecules into a zig-zag chain along the *c*-axis, Fig. 9b. The range of Hg–O bond lengths about the mercury atom spans nearly 0.75 Å, and the angles range from an acute 44º, formed by two bidentate nitrate-O atoms, to a wide 163º formed by the O atoms from two different nitrate ligands, thereby making assignment of a specific coordination geometry problematic.

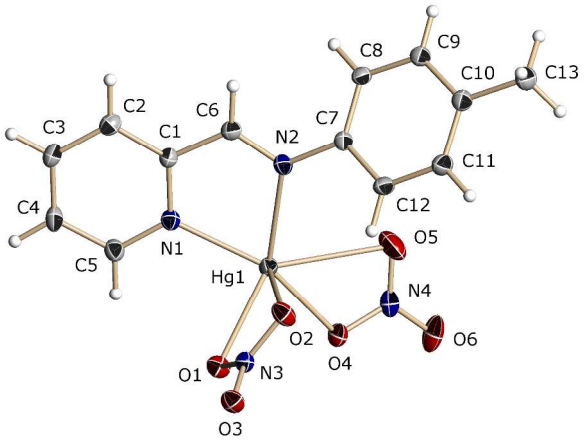

a)

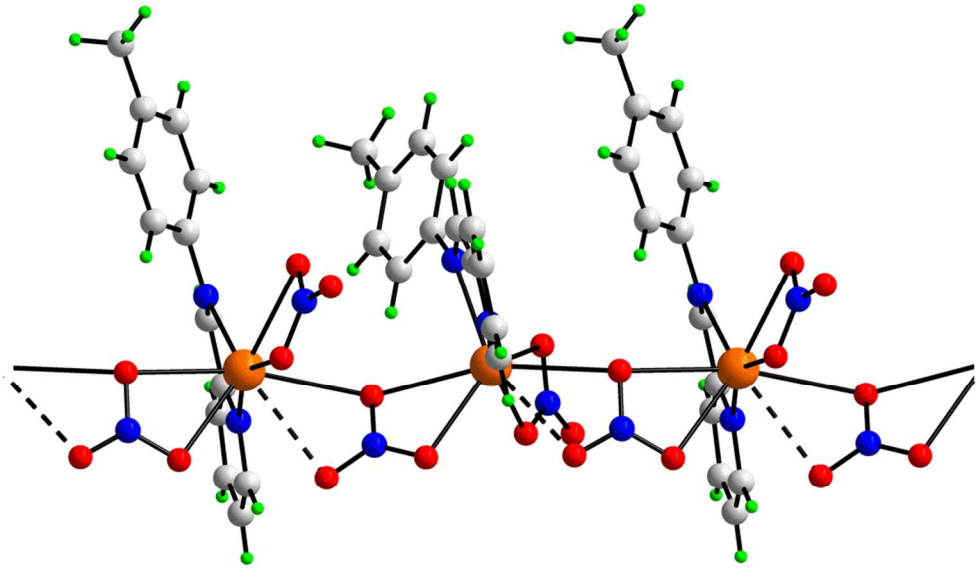

b)

Fig. 9 Perspective views of $[Hg(NO_3)_2L^4]$: (a) the asymmetric unit, and (b) the $[Hg(NO_3)_2L^4]_n$ chains found in the crystal structure of compound **9**. The displacement ellipsoids for a) are drawn at the 30% probability level and H atoms are shown as small spheres of arbitrary radii.

Table 4 Selected bond lengths (Å) and angles (º) for **9**

Parameter		Parameter	
Hg1–N1	2.218(4)	Hg1–O3^{i}	2.913(3)
Hg1–N2	2.353(3)	N1–C1	1.351(5)
Hg1–O1	2.534(3)	N1–C5	1.340(5)
Hg1–O2	2.620(3)	N2–C6	1.276(5)
Hg1–O4	2.174(3)	N2–C7	1.438(5)
Hg1–O5	2.739(4)	C1–C6	1.473(6)
Hg1–O2^{i}	2.755(3)		
N1–Hg1–N2	73.13(12)	N1–Hg1–O1	87.86(11)
N1–Hg1–O2	102.81(12)	N1–Hg1–O4	152.22(12)
N1–Hg1–O5	141.44(14)	N1–Hg1–O2^{i}	81.42(11)
N1–Hg1–O3^{i}	80.87(11)	N2–Hg1–O1	125.05(11)
N2–Hg1–O2	84.53(11)	N2–Hg1–O4	131.90(12)
N2–Hg1–O5	84.14(12)	N2–Hg1–O2^{i}	112.33(11)
N2–Hg1–O3^{i}	148.52(11)	O1–Hg1–O2	49.52(10)
O1–Hg1–O4	85.03(11)	O1–Hg1–O5	130.57(13)
O1–Hg1–O2^{i}	115.03(10)	O1–Hg1–O3^{i}	70.12(9)
O2–Hg1–O4	92.82(12)	O2–Hg1–O5	105.59(13)
O2–Hg1–O2^{i}	163.04(13)	O2–Hg1–O3^{i}	118.94(9)
O4–Hg1–O5	50.35(12)	O4–Hg1–O2^{i}	77.41(12)
O4–Hg1–O3^{i}	71.46(11)	O5–Hg1–O2^{i}	78.99(13)
O5–Hg1–O3^{i}	106.81(11)	O2^{i}–Hg1–O3^{i}	44.93(9)
Hg1–N1–C1	116.7(3)	Hg1–N1–C5	124.2(3)
Hg1–N2–C6	112.3(3)	Hg1–N2–C7	125.8(3)
Hg1–O1–N3	98.6(2)	Hg1–O2–N3	93.8(2)
Hg1–O4–N4	108.7(3)	Hg1–O5–N4	83.0(3)
Hg1^{ii}–O2–N3	97.5(2)	Hg1^{ii}–O3–N3	91.0(2)
Hg1–O2–Hg^{ii}	149.38(16)		

Symmetry operators for primed atoms: *i: x*, -*y*+1/2, *z*+1/2; *ii: x*, -*y*+1/2, *z*-1/2

Before describing the salient feature of the crystal packing of **1**-**10** , a few general observations based on the literature structures containing L^1-L^4 should be made. A survey of the Cambridge Crystallographic Database[85] revealed 25 structures with L^1, 2 each containing L^2 and L^3, and 18 examples of structures having L^4. In each case, $L^{1\text{-}4}$ was present as a chelating ligand. There are two closely related structures particularly worthy of special mention. While the structure of $[ZnI_2L^1]$[86] resembles that of mononuclear $[HgI_2L^1]$ (**3**), by contrast, the structure of $[ZnCl_2L^1]$[87] is mononuclear compared with binuclear $[HgCl_2L^1]_2$ (**1**), a result correlated with the reduced Lewis acidity of zinc compared with mercury.

Crystal packing

In the absence of strong structure-directing hydrogen bonding, the crystal structures of **1**-**10** may be considered as close packing of the various supramolecular zero- and one-dimensional aggregates. Despite the close similarity of the molecular structures, with the exception of **1**[48] and **2** pair, none of the structures are isomorphous. The crystal packing patterns are discussed in the same order as for the molecular structures, *i.e.* generally in order of increasing nuclearity of the molecular aggregates.

The crystal structure of **3** comprises loosely associated dimers of **3** held together by π···π interactions [3.705(2) Å] formed between the pyridyl and benzene rings as detailed in ESI Fig. S6. The dimers stack in columns along the *b*-axis with no specific interactions between them. To a first approximation, a similar situation pertains in the crystal structure of **8** with an important difference in that the columns of loosely associated dimers found in **3** are now connected into supramolecular chains along the *b*-axis by π···π interactions occurring between the chelate and pyridyl rings, as illustrated in Fig. 10; geometric details characterising these interactions are

given in the Figure caption. While not often commented upon, intermolecular interactions involving chelate rings, having metalloaromatic character,[88] interacting with other chelate rings, other aromatic rings, and as both acceptors and donors of C–H contacts are attracting increasing attention in the supramolecular chemistry literature.[89] The formation of $\pi(HgN_2C_2)\cdots\pi$(pyridyl) interactions in **8** but not in **3** is correlated with the better coordinating ability of L^4 compared with L^1, as commented upon above.

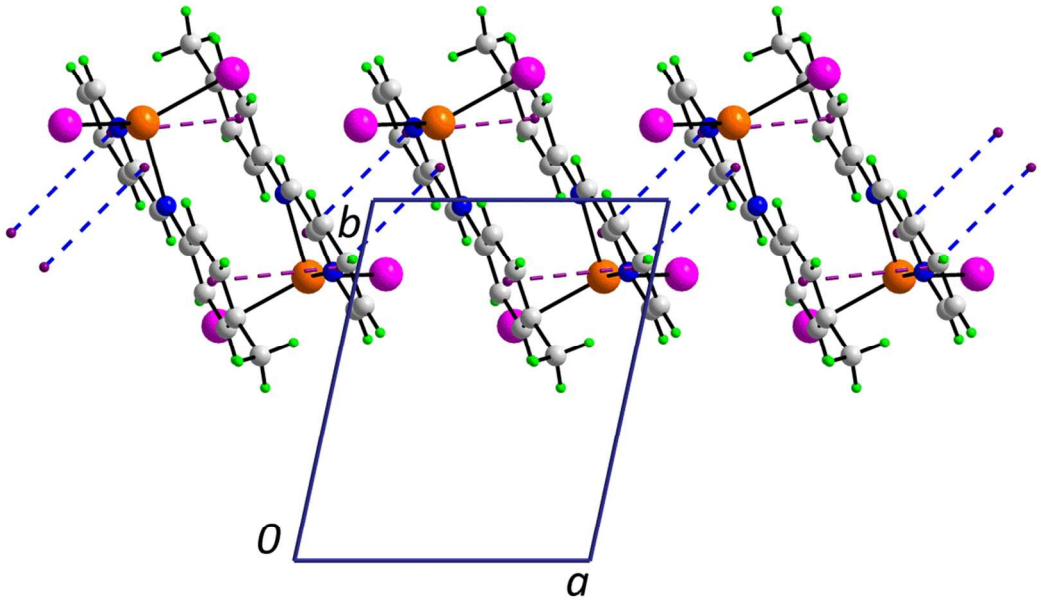

Fig. 10 Unit cell contents for **8** viewed in projection down the *c*-axis. The $\pi\cdots\pi$ interactions between the (N1,C1-C5) and $(C7\text{-}C12)^{i}$ rings are indicated as purple dashed lines [inter-centroid distance = 3.739(4) Å, angle of inclination between the rings = 4.9(3)º for symmetry operation *i*: 1-*x*, 2-*y*, 2-*z*] and those formed between the chelate ring, HgN_2C_2, and $(N1,C1\text{-}C5)^{ii}$ shown as blue dashed lines [inter-centroid distance = 3.703(4) Å, angle of inclination = 4.5(3)º for *ii*: 2-*x*, 2-*y*, 2-*z*].

Just as the mononuclear arrangement in **3** was transformed into a binuclear unit in **2** was correlated with the increase in electronegativity of Br compared with I, the presence of π(HgN$_2$C$_2$)···π(pyridyl) interactions in **2** but not in **3** is due to the same reason: the electronegativity difference enhances the metalloaromatic behaviour of the chelate ring. Owing to the binuclear nature of the molecules in **2**, layers mediated by these interactions are formed in the *ab*-plane with additional stabilisation provided by C–H···Br interactions, Fig. 11. A similar layer arrangement is seen in the crystal structure of **7**, ESI Fig. S8, but the chelate rings are interacting with the C$_6$ rather than the pyridyl rings of L[4], and additional stabilization by methyl-C–H···π(pyridyl) interactions is noted.

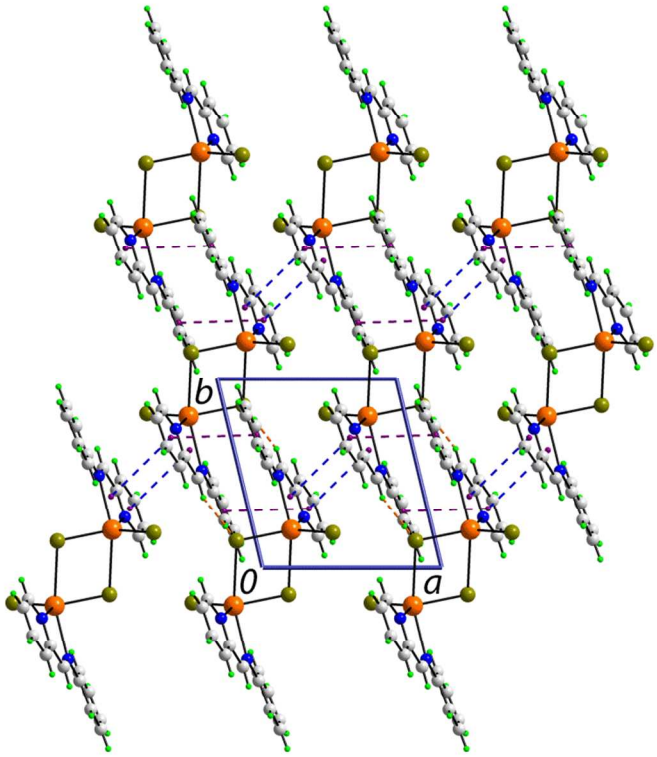

Fig. 11 Supramolecular layer in the *ab*-plane in **2**. The π···π interactions between the (N1,C1-C5) and (C7-C12)^{i} rings are indicated as purple dashed lines [inter-centroid distance = 3.820(4) Å, angle of inclination between the rings = 9.7(3)° for symmetry operation *i*: -*x*,1-*y*,-*z*] and those

formed between the chelate ring, HgN_2C_2, and (N1,C1-C5)^{ii} are shown as blue dashed lines [inter-centroid distance = 3.764(3) Å, angle of inclination = 4.4(3)º for *ii*: 1-*x*,1-*y*,-*z*]. The C6–H6···Br1^{iii} contacts are shown as orange dashed lines [H6···Br1^{iii} = 2.92 Å, C6...Br1^{iii}= 3.800(6) Å and angle at H6 = 155º for *iii*: -*x*,1-*y*,-*z*].

The crystal structure of **1**[48] is isomorphous with **2**. While on electronic grounds, greater metalloaromaticity is anticipated in the polymorphic $[HgX_2L^2]_2$ structures **4a** and **4b**, these are not found owing to the significant deviations from planarity of the L^2 ligands which preclude close approach of the chelate rings. In **4a**, the molecules are connected by pyridyl-C–H···Cl and π···π interactions, with the latter occurring between pyridyl and tolyl rings, see ESI Fig. S9. In **4b**, the π···π interactions occur exclusively between pyridyl rings, while the pyridyl-C–H···Cl contacts persist, see ESI Fig. S10. With no steric hindrance in **5**, chelate rings again feature in the supramolecular assembly. In this case, the molecules are arranged to allow the chelate rings to self-associate *via* π···π interactions, see Fig. 12. The resulting aggregates are connected into a supramolecular layer *via* π···π interactions occurring between pyridyl rings. With the foregoing in mind, perhaps contrary to expectation, the binuclear molecules in **6** aggregate into a three-dimensional architecture *via* π···π interactions occurring between pyridyl and C_6 rings as well as pyridyl-C–H···Cl interactions with no evidence for participation in intermolecular interactions by the chelate rings, see ESI. Fig. 11.

The supramolecular chains in **10** are consolidated in the crystal packing by a combination of π···π interactions, occurring between pyridyl and C_6 rings, as well as C–H···N interactions, see ESI Fig. 12. Finally, and in contrast to the packing features described thus far, the crystal

structure of **9** is devoid of π···π interactions with the supramolecular chains sustained in a three-dimensional architecture by a network of C–H···O interactions, see ESI Fig. 13.

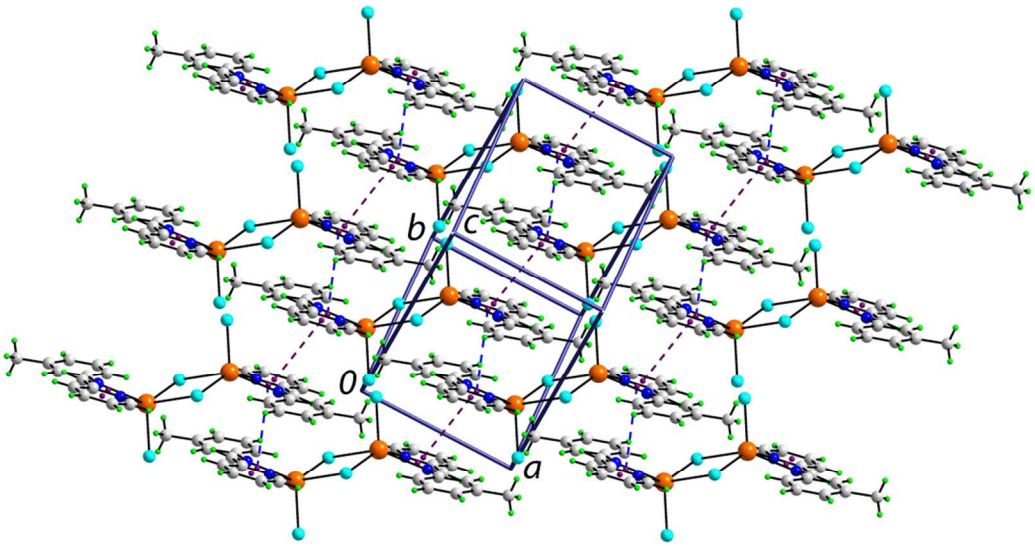

Fig. 12 Supramolecular layer approximately parallel to (0 -1 6) in **5**. The π···π interactions between the (N1,C1-C5) and (N1,C1-C5)^{i} rings are indicated as purple dashed lines [inter-centroid distance = 3.784(3) Å, angle of inclination between the rings = 0º for symmetry operation *i*: 1-*x*,-*y*,-*z*] and those formed between the chelate rings are shown as blue dashed lines [inter-centroid distance = 3.851(2) Å, angle of inclination = 0º for *ii*: 1-*x*, 1-*y*,-*z*].

Conclusions

The synthesis and structural characterization of a series of mercury complexes with (*E*)-*N*-(pyridin-2-ylmethylene)arylamine (Chart 1), which differ in the location of the substituent in the aryl ring, and in the type of the counter ion has been achieved. These assemble to generate four types of neutral complexes of formulae: zero-dimensional HgX_2L (**3**, **8**), $[HgX_2L]_2$ (**1**, **2**, **4**-**7**), and one dimensional $[Hg(NO_3)_2L]_n$ (**9**) and $\{[Hg(N_3)_2L]_2\}_n$ (**10**) depending on the bridging

capacity of the counter ion. The propensity for the formation of self-assembled binuclear entities over mononuclear species in the sequence Cl > Br > I and is related to the electronegativity of X. The influence of the presence (and position) of the methyl group in the (*E*)-*N*-(pyridin-2-ylmethylene)arylamine ligands can promote the formation of π...π interactions involving the five-membered chelate rings in supramolecular assembly.

Acknowledgments

The financial support of the Department of Science & Technology, New Delhi, India (Grant No.SR/S1/IC-03/2005,TSBB), the University Grants Commission, New Delhi, India, through SAP-DSA, Phase-III and Indo-Swiss Joint Research Programme, Joint Utilisation of Advanced Facilities (Grant No. JUAF 11, TSBB, AL) are gratefully acknowledged. Support from the Ministry of Higher Education, Malaysia, High-Impact Research scheme (UM.C/HIR-MOHE/SC/03) is also gratefully acknowledged.

References

1 W. Kaim and B. Schwederski, *Bioinorganic Chemistry: Inorganic Elements in the Chemistry of Life*, Wiley, Chichester, 1996.

2 A. Morsali and M. Y. Masoomi, *Coord. Chem. Rev*., 2009, **253**, 1882-1905.

3 M. A. Pitt and D. W. Johnson, *Chem. Soc. Rev*., 2007, **36**, 1441-1453.

4 G. Mahmoudi, A. Morsali and L. G. Zhu, *Polyhedron*, 2007, **26**, 2885-2893.

5 G. Mahmoudi and A. Morsali, *CrystEngComm,* 2007, **9**, 1062-1072

6 Y. G. Ma, C. M. Che, H. Y. Chao, X. M. Zhou, W. H. Chan and J. C. Shen, *Adv. Mater*., 1999, **11**, 852-857.

7 X. M. Zhang, M. L. Tong, M. L. Gong, H. K. Lee, L. Luo, K. F. Li, Y. X. Tong and X. M. Chen, *Chem. Eur. J*., 2002, **8**, 3187-3194.

8 G. Yu, S. W. Yin, Y. Q. Liu, Z. G. Shuai and D. B. Zhu, *J. Am. Chem. Soc*., 2003, **125**, 14816-14824.

9 W. K. Lo, W. K. Wong, W. Y. Wong and J. P. Guo, *Eur. J. Inorg. Chem.* 2005, 3950-3954.

10 M. R. Haneline, M. Tsunoda and F. P. Gabbai, *J. Am. Chem. Soc.*, 2002, **124**, 3737-3742.

11 R. Q. Fan, D. S. Zhu, Y. Mu, G. H. Li, Y. L. Yang and Q. Su, *Eur. J. Inorg. Chem.*, 2004, 4891-4897.

12 V. W. W. Yam, K. K. W. Lo, W. K. M. Fung and C. R. Wang, *Coord. Chem. Rev*., 1998, **171**, 17-41.

13 H. H. Patterson, S. M. Kanan and M. A. Omary, *Coord. Chem. Rev*., 2000, **128**, 227-241.

14 F. Li, M. Zhang, G. Cheng, J. Feng, Y. Zhao, Y. G. Ma, S. Y. Liu and J. C. Shen, *Appl. Phys. Lett*., 2004, **84**, 148-150.

15 Y. K. Chan, P. K. Ng, X. Gong and S. J. Hou, *Appl. Phys. Lett*., 1999, **75**, 3920-3922.

16 K. Z. Wang, L. Huang, L. H. Gao, L. P. Jin and C. H. Huang, *Inorg. Chem*., 2002, **41**, 3353-3358.

17 S. Ranjan, S. Y. Lin, K. C. Hwang, Y. Chi, W. L. Ching, C. S. Liu, Y. T. Tao, C. H. Chien, S. M. Peng and G. H. Lee, *Inorg. Chem*., 2003, **42**, 1248-1255.

18 Y. L. Tung, S. W. Lee, Y. Chi, L. S. Chen, C. F. Shu, F. I. Wu, A. J. Carty, P. T. Choi, S. M. Peng and G. H. Lee, *Adv. Mater*., 2005, **17**, 1059-1064.

19 H. Xia, C. Zhang, X. Liu, S. Qiu, P. Lu, F. Shen, J. Zhang and Y. Ma, *J. Phys. Chem.*, *B*, 2004, **108**, 3185-3190.

20 H. Xia, C. Zhang, X. Liu, S. Qiu, P. Lu, J. Zhang and Y. Ma, *Appl. Phys. Lett*., 2004, **84**, 290-292.

21 B. Carlson, G. D. Phelan, W. Kaminsky, L. Dalton, X. Z. Jiang, S. Liu and A. K.-Y. Jen, *J. Am. Chem. Soc*., 2002, **124**, 14162-14172.

22 Y. L. Chen, S. W. Lee, Y. Chi, K. C. Hwang, S. B. Kumar, Y. H. Hu, Y. M. Cheng, P. T. Chou, S. M. Peng, G. H. Lee, S. J. Yeh and C. T. Chen, *Inorg. Chem*., 2005, **44**, 4287-4294.

23 Y. L. Tung, P. C. Wu, C. S. Liu, Y. Chi, J. K. Yu, Y. H. Hu, P. T. Chou, S. M. Peng, G. H. Lee, Y. Tao, J. C. Arthur, C. F. Shu and F. I. Wu, *Organometallics*, 2004, **23**, 3745-3748.

24 W.-Y. Wong, G.-L. Lu, L. Liu, J.-X. Shi and Z. Lin, *Eur. J. Inorg. Chem*., 2004, 2066-2077.

25 X.-M. Liu, X.-Y. Mu, H. Xia, L. Ye, W. Gao, H.-Y. Wang and Y. Mu, *Eur. J. Inorg. Chem*., 2006, 4317-4323.

26 W.-Y. Wong, *Coord. Chem. Rev*., 2007, **251**, 2400-2427.

27 S. J. Faville, W. Henderson, T. J. Mathienson and B. K. Nicholson, *J. Organomet. Chem*., 1999, **580**, 363-369.

28 W.-Y. Wong, L. Liu and J.-X. Shi, *Angew. Chem., Int. Ed. Engl*., 2003, **42**, 4064-4068.

29 R. J. Puddephatt, *Chem. Commun*., 1998, pp. 1055-1062.

30 R. J. Puddephatt, *Coord. Chem. Rev*., 2001, **216-217**, 313-332.

31 H. Schmidbaur, *Chem. Soc. Rev*., 1995, **24**, 391-400.

32 C.-M. Che, H.-Y. Chao, V. M. Miskowski, Y. Li and K.-K. Cheung, *J. Am. Chem. Soc*., 2001, **123**, 4985-4991.

33 W. Lu, H.-F. Xiang, N. Zhu and C.-M. Che, *Organometallics*, 2002, **21**, 2343-2346.

34 H.-Y. Chao, W. Lu, Y. Li, M. C. W. Chan, C.-M. Che, K.-K. Cheung and N. Zhu, *J. Am. Chem. Soc*., 2002, **124**, 14696-14706.

35 M. I. Bruce, B. C. Hall, B. W. Skelton, M. E. Smith and A. H. White, *J. Chem. Soc., Dalton Trans*., 2002, 995-1001.

36 P. Li, B. Ahrens, K.-H. Choi, M. S. Khan, P. R. Raithby, P. J. Khan, M. S. Wilson and W.-Y. Wong, *CrystEngComm*, 2002, **4**, 405-412.

37 B. C. Tzeng, A. Schier and H. Schmidbaur, *Inorg. Chem*., 1999, **38**, 3978-3984.

38 B. C. Hollatz, A. Schier and H. Schmidbaur, *J. Am. Chem. Soc*., 1997, **119**, 8115-8116.

39 E. R. T. Tiekink and J.-G. Kang, *Coord. Chem*. *Rev*., 2009, **253**, 1627-1648.

40 M. J. Irwin, J. J. Vittal and R. J. Puddephatt, *Organometallics*, 1997, **16**, 3541-3547.

41 W. J. Hunks, M. A. MacDonals, M. C. Jennings and J. Puddephatt, *Organometallics*, 2000, **19**, 5063-5070.

42 I. Persson, M. Sandstrom, P. L. Goggin and A. Mosset, *J. Chem.Soc., Dalton Trans.,* 1985, pp. 1597-1604 (and references therein).

43 C. Hu, I. Kalf and U. Englert, *CrystEngComm*., 2007, **9**, 603-610.

44 (a) J. E. Huheey, *Anorganische Chemie*, de Gruyter, Berlin, New York, 1988; (b) G. Schwarzenbach and M. Schellenberg, *Helv. Chim. Acta,* 1965, **48**, 28-46.

45 E. Freire, S. Baggio, R. Baggio and L. Suescun, *J. Chem. Cryst*., 1999, **29**, 825-830.

46 F. Ramezanipour, H. Aghabozorga and J. Soleimannejad, *Acta Crystallogr., Sect. E: Struct. Rep. Online*, 2005, **61**, m1194-m1196.

47 T. S. Basu Baul, A. Lycka, R. Butcher and F. E. Smith, *Polyhedron*, 2004, **23**, 2323-2329.

48 M. F. Nejad, M. R. T. B. Olyai and H. R. Khavasi, *Z. Kristallogr. New Cryst. Struct.,* 2010, **225,** 717-718.

49 A. J. Bloodworth, *J. Organomet. Chem*., 1970, **23**, 27-30.

50 N. S. Moyon and S. Mitra, *J. Phys. Chem.; B,* 2011, **115**, 10163-10172.

51 M. Wiebcke, D. Mootz, *Acta Crystallogr., Sect. B: Struct. Sci*., 1982, **38**, 2008-2013.

52 M. J. Frisch, G. W. Trucks, H. B. Schlegel, G. E. Scuseria, M. A. Robb, J. R. Cheeseman, J. A. Montgomery Jr, T. Vreven, K. N. Kudin, J. C. Burant, J. M. Millam, S. S. Iyengar, J. Tomasi, V. Barone, B. Mennucci, M. Cossi, G. Scalmani, N. Rega, G. A. Petersson, H. Nakatsuji, M. Hada, M. Ehara, K. Toyota, R. Fukuda, J. Hasegawa, M. Ishida, T. Nakajima, Y. Honda, O. Kitao, H. Nakai, M. Klene, X. Li, J. E. Knox, H. P. Hratchian, J. B. Cross, V. Bakken, C. Adamo, J. Jaramillo, R. Gomperts, R. E. Stratmann, O. Yazyev, A. J. Austin, R. Cammi, C. Pomelli, J. W. Ochterski, P. Y. Ayala, K. Morokuma, G. A. Voth, P. Salvador, J. J. Dannenberg, V. G. Zakrzewski, S. Dapprich, A. D. Daniels, M. C.

Strain, O. Farkas, D. K. Malick, A. D. Rabuck, K. Raghavachari, J. B. Foresman, J. V. Ortiz, Q. Cui, A. G. Baboul, S. Clifford, J. Cioslowski, B. B. Stefanov, G. Liu, A. Liashenko, P. Piskorz, I. Komaromi, R. L. Martin, D. J. Fox, T. Keith, M. A. Al-Laham, C. Y. Peng, A.Nanayakkara, M. Challacombe, P. M. W. Gill, B. Johnson, W. Chen, M. W. Wong, C. Gonzalez, J. A. Pople, *Gaussian 03, Revision D.01*, Gaussian, Inc., Wallingford, CT, **2004**.

53 T. S. Basu Baul, P. Das, A. K. Chandra, S. Mitra and S. M. Pyke, *Dyes Pigments*, 2009, **82**, 379-386.

54 M. P. Andersson and P. Uvdal, *J. Phys. Chem., A*, 2005, **109**, 2937-2941.

55 R. Hooft, *KappaCCD Collect Software*, Nonius BV, Delft, The Netherlands, 1999.

56 *CrysAlisPro*, Version 1.171.33.55, Agilent Technologies, Yarnton, Oxfordshire, England, 2010.

57 Z. Otwinowski, W. Minor, In *Methods in Enzymology*, (C. W. Carter Jr. and R. M. Sweet ed.), vol. 276, Macromolecular Crystallography, Part A, Academic Press, New York, 1997, pp. 307-326.

58 *Bruker Analytical X-ray Systems*, SAINT-NT Version 6.04, 2001.

59 R. H. Blessing, *Acta Crystallogr*., *Sect. A, Foundat. Crystallogr.,* 1995, **51**, 33-38.

60 R. C. Clark and J. S. Reid, *Acta Crystallogr*., *Sect. A, Foundat. Crystallogr.,* 1995, **51**, 887-897.

61 P. T. Beurskens, G. Admiraal, G. Beurskens, W. P. Bosman, S. Garcia-Granda, R. O. Gould, J. M. M. Smits and C. Smykalla, *PATTY: The DIRDIF Program System*, Technical Report of the Crystallography Laboratory, University of Nijmegen, The Netherlands, 1992.

62 P. T. Beurskens, G. Admiraal, G. Beurskens, W. P. Bosman, R. de Gelder, R. Israel and J. M. M. Smits, *DIRDIF94: The DIRDIF Program System*, Technical Report of the Crystallography Laboratory, University of Nijmegen, The Netherlands, 1994.

63 G. M. Sheldrick, *Acta Crystallogr*., *Sect. A, Foundat. Crystallogr.*, 2008, **64**, 112-122.

64 A. Altomare, G. Cascarano, C. Giacovazzo, A. Guagliardi, M. C. Burla, G. Polidori and M. Camalli, *SIR92*, *J. Appl. Crystallogr.,* 1994, **27**, 435-436.

65 *Bruker Analytical X-ray Systems*, SHELXTL-NT Version 6.10, 2000.

66 S. S. Tandon, S. Chander and L. K. Thompson, *Inorg. Chim. Acta*, 2000, **300-302**, 683-692.

67 K. Nakamoto, *Infrared and Raman Spectra of Inorganic and Coordination Compounds*, Wiley, New York, 1986.

68 G. Mahmoudi and A. Morsali, *Polyhedron*, 2008, **27**, 1070-1078.

69 G. J. Kleywegt, W. R. Wiesmeijer, G. J. Van Driel, W. L. Driessen and J. Reedijk, *J. Chem. Soc., Dalton Trans*., 1985, 2177-2184.

70 A. K. Boudalis, V. Nastopoulos and S. P. Perlepes, *Trans. Met. Chem*., 2001, **26**, 276-281.

71 J. Ribas, A. Escuer, M. Monfort, R. Vicente, R. Cortes, L. Lezama and T. Rojo, *Coord. Chem. Rev*., 1999, **193-195**, 1027-1068.

72 U. S. Ray, B. G. Chand, G. Mostafa, J. Cheng, T.-H. Lu and C. Sinha, *Polyhedron*, 2003, **22**, 2587-2594.

73 T. K. Chattopadhyay, A. K. Kumar, A. Roy, A. S. Batsanov, E. B. Shamuratov, Yu. T. Struchkov, *J. Organomet. Chem.,* 1991, **419**, 277-282.

74 S. Basu Baul, T. S. Basu Baul, E. Rivarola, D. Dakternieks, E. R. T. Tiekink, A. Chatterjee and C. Sing-ai, *Appl. Organometal. Chem*., 1998, **12**, 503-513.

75 B. Chand, U. Ray, P. K. Santra, G. Mostafa, T.-H. Lu and C. Sinha, *Polyhedron*, 2003, **22**, 1205-1212.

76 B. G. Chand, U. S. Ray, G. Mostafa, J. Cheng, T.-H. Lu and C. Sinha, *Inorg. Chim. Acta*, 2005, **358**, 1927-1933.

77 C. Seward, J. Chan, D. Song and S.-N. Wang, *Inorg. Chem*., 2003, **42**, 1112-1120.

78 (a) R. S. Drago, *Physical Methods in Chemistry*, Ch. 5, W. B. Saunders Company, Philadelphia 1977; (b) F. Masetti, U. Mazzucato and G. Galiazzo, *J. Lumin*., 1971, **4**, 8-12; (c) T. C. Warner, W. Hawkins, J. Facci, R. Torrisi and T. Trembath, *J. Phys. Chem*., 1978, **82**, 298-301; (d) M. C. Aragoni, M. Arca, F. Demartin, F. A. Devillanova, F. Isaia, A. Garau, V. Lippolis, F. Jalali, U. Papke, M. Shamsipur, L. Tei, A. Yari and G. Verani, *Inorg. Chem*., 2002, **41**, 6623-6632.

79 (a) P. L. Ng, C. S. Lee, H. L. Kwong and A. S. C. Chan, *Inorg. Chem. Commun*., 2005, **8**, 769-772; (b) B. Xiao, H. W. Hou, Y. T. Fan and M. S. Tang, *Inorg. Chim. Acta*, 2007, **360**, 3019-3025.

80 G. Mahmoudi, S. Rafiei, A. Morsali and L.-G. Zhux, *J. Coord. Chem.,* 2008, **61**, 789-795.

81 A. Bondi, *J. Phys. Chem.*, 1964, **68**, 441-452.

82 A. W. Addison, T. N. Rao, J. Reedijk, J. van Rijn and G. C. Verschoor, *J. Chem. Soc. Dalton Trans*., 1984, pp. 1349-1356.

83 A. L. Spek, *Acta Crystallogr. Sect. D, Biol. Crystallogr*., 2009, **65**, 148-155.

84 J. Gans and D. Shalloway, *J. Molec. Graphics Model*., 2001, **19**, 557-559.

85 F. H. Allen, *Acta Crystallogr., Sect. B: Struct. Sci*., 2002, **58**, 380-388.

86 K. Wurst and M. R. Buchmeiser, *Heterocyclic Commun*., 1999, **5**, 37-44.

87 (a) M. Schulz, M. Klopfleisch, H. Gorls, M. Kahnes and M. Westerhausen, *Inorg. Chim. Acta*, 2009, **362**, 4706-4712; (b) J. J. Braymer, J.-S. Choi, A. S. DeToma, C. Wang, K. Nam, J. W. Kampf, A. Ramamoorthy and M. H. Lim, *Inorg.Chem*., 2011, **50**, 10724-10734.

88 (a) H. Masui, *Coord. Chem. Rev*., 2001, **219–221**, 957-992; (b) Y. Z. Wang and G. H. Robinson, *Organometallics*, 2007, **26**, 2-11.

89 (a) Z. D. Tomić, D. N. Sredojević and S. D. Zarić, *Cryst. Growth Des*., 2006, **6**, 29-31; (b) D. N. Sredojević, Z. D. Tomić and S. D. Zarić, *Cryst. Growth Des*., 2010, **10**, 3901-3908; (c) M. K. Milčič, V. B. Medaković, D. N. Sredojević, N. O. Juranić and S. D. Zarić, *Inorg. Chem*., 2006, **45**, 4755-4763; (d) E. R. T. Tiekink and J. Zukerman-Schpector, *Chem. Commun.*, 2011, **47**, 6623-6625; (e) E. R. T. Tiekink, Crystal Engineering. in Supramolecular Chemistry: from Molecules to Nanomaterials, J. W. Steed and P.A. Gale (eds). John Wiley & Sons Ltd, Chichester, UK, 2012, pp. 2791-2828.

The influence of counter ion and ligand methyl substitution on the solid-state structures and photophysical properties of mercury(II) complexes with (E)-N-(pyridin-2-ylmethylene)arylamines†

Tushar S. BasuBaul,*[a] Sajal Kundu,[a] Sivaprasad Mitra,[a] Herbert Höpfl,[b] Edward R. T. Tiekink,*[c] Anthony Linden[d]

Supramolecular aggregation and solution-state photophysical properties of Hg((*E*)-*N*-(pyridin-2-ylmethylene)arylamine) complexes is shown to be dependent on the nature of the counter-anions {Cl, Br, I, N_3 and NO_3}.